Functional identification of soluble uric acid as an endogenous inhibitor of CD38

Shijie Wen[1], Hiroshi Arakawa[1*], Shigeru Yokoyama[2,3], Yoshiyuki Shirasaka[1], Haruhiro Higashida[2], Ikumi Tamai[1,4*]

[1]Faculty of Pharmaceutical Sciences, Institute of Medical, Pharmaceutical and Health Sciences, Kanazawa University, Kanazawa, Japan

[2]Research Center for Child Mental Development, Kanazawa University, Kanazawa, Japan

[3]Division of Socio-Cognitive-Neuroscience, United Graduate School of Child Development, Osaka University, Kanazawa University, Hamamatsu University School of Medicine, Chiba University and University of Fukui, Kanazawa, Japan

[4]Lead contact

[*]Correspondence: tamai@p.kanazawa-u.ac.jp (I.T.), arakawa@p.kanazawa-u.ac.jp (H.A.).

Abstract

Excessive elevation or reduction of soluble uric acid (sUA) levels has been linked to some of pathological states, raising another subject that sUA at physiological levels may be essential for the maintenance of health. Yet, the fundamental physiological functions and molecular targets of sUA remain largely unknown. Using enzyme assays and *in vitro* and *in vivo* metabolic assays, we demonstrate that sUA directly inhibits the hydrolase and cyclase activities of CD38 via a reversible non-competitive mechanism, thereby limiting nicotinamide adenine dinucleotide (NAD^+) degradation. CD38 inhibition is restricted to sUA in purine metabolism, and a structural comparison using methyl analogs of sUA such as caffeine metabolites shows that 1,3-dihydroimidazol-2-one is the main functional group. Moreover, sUA at physiological levels prevents crude lipopolysaccharide (cLPS)-induced systemic inflammation and monosodium urate (MSU) crystal-induced peritonitis in mice by interacting with CD38. Together, this study unveils an unexpected physiological role for sUA in controlling NAD^+ availability and innate immunity through CD38 inhibition, providing a new perspective on sUA homeostasis and purine metabolism.

Key Words

uric acid, MSU crystal, CD38, nicotinamide adenine dinucleotide, inflammation, innate immunity, hyperuricemia, hypouricemia, gout, metabolism

Introduction

The evolutionary loss of uricase activity in humans and certain primates completely blocks the degradation of soluble uric acid (sUA), leading to higher physiological levels of sUA than in other mammals (1, 2). Owing to renal reabsorption, sUA is strictly maintained in humans rather than being eliminated as a waste. It has been suggested that sUA functions as an abundant antioxidant (3) and is crucial to maintain blood pressure (4). Although hyperuricemia may promote the precipitation of monosodium urate (MSU) crystal, an activator of the NLRP3 inflammasome (5), resulting in diseases such as gout (6) and kidney stone disease (7), numerous studies have indicated the protective potential of sUA in neurodegenerative diseases (8-10). In addition, abnormal reduction of sUA levels is clinically associated with the risk of various diseases (9, 11), including cardiovascular diseases and kidney diseases. Intriguingly, rapid urate reduction in the initiation of therapy even increases gout flares in patients (12). Depletion of sUA in uricase-transgenic mice shortens lifespan and promotes sterile inflammation induced by microbial molecules or pro-inflammatory particles (13, 14). Thus, data support that sUA provides physiological defense against excessive inflammation, aging, and certain diseases (9, 11, 15-20). However, the underlying molecular basis of sUA physiology remains poorly understood.

To gain insight into target-based physiological functions of sUA, our laboratory utilized magnetic bead-conjugated 8-oxoguanine (8-OG, an sUA analog; technically, sUA cannot be directly conjugated to the beads) and proteomic analysis to screen the potential candidates of sUA-binding proteins. We discovered several binding proteins of 8-OG (unpublished data), including CD38 that was verified by enzyme inhibition (Figure 1A), which raised our interest in exploring the role of CD38 in sUA physiology. CD38 is mainly expressed in immune cells and functions as a hydrolase to degrade nicotinamide adenine dinucleotide (NAD^+) (21), an essential cofactor for various metabolic reactions that sustain life (22), thus regulating inflammation, aging, and various diseases (21, 23). Its cyclase catalyzes the synthesis of cyclic ADP-ribose (cADPR) from NAD^+ to drive calcium mobilization (24, 25), which is crucial for social

behavior (26) and neutrophil recruitment (27).

Here, we demonstrate that sUA at physiological levels directly inhibits CD38 and consequently limits NAD^+ degradation and excessive inflammation, which defines, for the first time, the physiological functions of sUA via CD38. In addition, we confirm the unique effect of sUA on CD38 in purine metabolism and identify a structural feature for pharmacological inhibition of CD38.

Results

sUA is an endogenous, reversible, and non-competitive inhibitor of CD38

To clarify whether CD38 is a direct target for sUA, we investigated the effect of sUA on CD38 activity. We found that sUA directly inhibited the hydrolase and cyclase activities of human (Figures 1B and S1B) and murine (Figure 1E) CD38 as a non-competitive inhibitor (Figures 1C, 1D, and S1A) with a K_i in the micromolar range (57.1- 93.3 μM), demonstrating its binding to the allosteric sites of CD38. sUA showed comparable inhibitory effects on hydrolase and cyclase, as indicated by similar K_i. The physiological levels of sUA in humans (about 120-420 μM (28, 29)) and in several mouse tissues (Figure S1K) were higher than its K_i, indicating that human CD38 and murine type III/intracellular CD38 are physiologically inhibited by sUA. The inhibitory effects were reversible (Figures 1F, 1G, S1C and S1D), suggesting that sUA dynamically modulates CD38 activity. Interference from endogenous sUA was negligible when using tissues as an enzyme source, because the concentrations in the final reaction buffer were below 1 μM (Figure S1J).

CD38 inhibition is restricted to sUA in purine metabolism

Although the structure of sUA is similar to that of other purines, we confirmed its unique effect on CD38 in the major metabolic pathways of purines (Figure 2C). sUA precursors (adenosine, guanosine, inosine, hypoxanthine and xanthine) and the uricase-catalyzed metabolite (allantoin) hardly inhibited the hydrolase and cyclase activities of human (Figures 2A, 2B, and S1E) and murine (Figures S1F and S1G) CD38. The tested

purine concentrations were higher than their physiological levels (30-32). Thus, CD38 inhibition is restricted to sUA, suggesting a specific functional group in sUA.

To identify the functional group for CD38 inhibition, we tested additional xanthine analogs (oxypurinol and caffeine) and the methyl analogs (caffeine metabolites) of sUA including 1-methyluric acid (1-MU), 1,3-dimethyluric acid (1,3-DMU), 1,7-dimethyluric acid (1,7-DMU), and 1,3,7-trimethyluric acid (1,3,7-TMU). The results showed that only sUA analogs inhibited CD38 activity (Figure 2D). A structural comparison (Figure 2F) indicated that 1,3-dihydroimidazol-2-one (1,3-DHI-2-one) is the main functional group, as all other purines lacking this group failed to inhibit CD38 activity. In addition, the ring-opening of the uracil group after sUA conversion to allantoin abrogated this inhibitory potential. Uracil or 1,3-dihydroimidazol-2-one (Figures 2E, S1H, and S1I) alone did not affect CD38 activity. Therefore, the adjacent uracil-like heterocycles are also essential for CD38 inhibition.

sUA at physiological levels limits NAD^+ degradation by directly inhibiting CD38

Next, we explored the effect of sUA on NAD^+ availability, as CD38 is a key enzyme in degrading NAD^+ and its precursor, nicotinamide mononucleotide (NMN) (33). sUA boosted intracellular NAD^+ in A549 and THP-1 cells (Figures S3A and S3B), then we investigated whether CD38 mediates the effect of sUA on NAD^+ degradation. Short-term and moderate "sUA-supplementation" model was constructed by gavage of inosine and oxonic acid (OA, an uricase inhibitor with a K_i in the nanomolar range (34)) in mice with "natural hypouricemia" (Figures 3D and S2C). The plasma sUA levels (around 120 μM) in our models were close to the minimum physiological concentrations in humans but were markedly lower than that in other long-term and hyperuricemia-associated disease models in rodents, which enabled us to evaluate the physiologically inhibitory effect of sUA on CD38 activity. Although OA was a weak inhibitor of CD38 with a IC_{50} in the millimolar range (Figures S1L and S1M), it seemed unlikely to affect CD38 activity in our models because of the incomplete inhibition of uricase, as evidenced by plasma sUA (Figure S1N). Although short-term administration

of OA alone failed to increase plasma sUA levels, we used it as the background for metabolic studies in mice to exclude potential interference.

One-day or 3-day moderate sUA supplementation slightly but significantly increased whole blood NAD^+ levels in wild-type (WT) mice but not in CD38 knockout (KO) mice (Figures 3A, 3D, S2C, and S2D). Similar results were also observed under inflammatory conditions (Figures S3C, S3D, S5D, and S5E). This indicates that CD38 mediates, at least in part, the suppressive effect of sUA on NAD^+ degradation. The suppression of NAD^+ degradation by the sUA-CD38 interaction was validated by a decrease in cADPR production under inflammatory conditions (Figure S3F) but not under non-inflammatory conditions (Figures 3C and S2F), possibly because of physiological compensation via other cADPR synthases. However, sUA had a minor effect on NMN levels *in vivo* (Figures 3B, S2E, S3E, and S5F), likely due to the rapid conversion of NMN to NAD^+ (35). Notably, WT and CD38 KO mice showed similar NAD^+ baselines in whole blood, suggesting that the metabolic background has been reprogrammed in CD38 KO mice; for instance, sirtuins with higher activity in CD38 KO mice (36) may consume more NAD^+. Moreover, sUA release *in vivo* showed that both plasma sUA and whole blood NAD^+ gradually returned to their initial levels (Figure 3E), which confirmed the reversible regulation of NAD^+ availability by sUA and excluded potential interference from epigenetic regulation of other bioconversion pathways of NAD^+. Metabolic assays using recombinant hCD38 further verified that increased NAD^+ availability is mediated by direct CD38-sUA interaction (Figure 3F).

In contrast, the tissue levels of NAD^+ and NMN were not increased in 1-day and 3-day sUA-supplementation models, probably because the tissue uptake of sUA was physiologically saturated before treatment (Figures S2A and S2B). The NAD^+ levels in the brain and heart appeared to be elevated in 7-day model (Figures S2G-S2I). Thus, the sUA-CD38 interaction in the circulation may indirectly increase tissue NAD^+ availability. Our models within 7 days did not show pro-inflammatory potential (Figure S7A), but we did not prolong the treatment time because long-term administration of

OA might induce renal damage with concomitant inflammation related to cell death.

Considering the rapid conversion of NMN to NAD^+ *in vivo*, we assessed the effect of sUA on extracellular NMN degradation *in vitro*. sUA directly inhibited NMN degradation by recombinant hCD38 (Figure S4A). Whereas sUA or other CD38 inhibitors failed to boost intracellular NAD^+ in primed WT bone marrow-derived macrophages (BMDMs) treated with NMN (Figure S4B). This is likely because another NAD^+-consuming enzyme, PARP1, is activated (37) and the NMN transporter expression is very low in BMDMs (33). Importantly, sUA increased extracellular NMN availability in WT BMDMs but not in CD38 KO BMDMs (Figures S4C and S4D). The addition of recombinant hCD38 restored the suppressive effect of sUA on extracellular NMN degradation in CD38 KO BMDMs (Figure S4E). Accordingly, sUA may also increase NAD^+ availability by inhibiting CD38-medaited NMN degradation.

sUA physiologically prevents excessive inflammation by interacting with CD38

NAD^+ is crucial for the activity of sirtuins that limit the NLRP3 inflammasome activation (38, 39), and cADPR may regulate calcium signaling to promote cytokine production (40, 41). Therefore, CD38 plays a key role in inflammation via NAD^+ metabolism (42). We confirmed the role of CD38 in the NLRP3 inflammasome activation. CD38 KO reduced IL-1β release driven by several inflammasome activators and the fungal component zymosan in primed BMDMs (Figure S6B). Pre-incubation with sUA at physiological or higher levels moderately suppressed inflammasome activation in primed THP-1 cells but not in primed WT BMDMs (Figures S6A and S6C). sUA uptake was very low in primed WT BMDMs (Figure S6E), suggesting a crucial role of intracellular sUA in regulating inflammasome activation *in vitro*. However, extracellular sUA may inhibit CD38-mediated NMN degradation to increase NAD^+ levels *in vivo*, thus limiting excessive inflammation via sirtuins signaling (38). Additionally, sUA did not induce IL-1β release in primed WT BMDMs and THP-1 cells (Figures S6A and S6D). These results argue against the pro-inflammatory potential of sUA (43) that has been challenged by the improper preparation of aqueous solution

(MSU crystal precipitation) in basic studies (44, 45). In fact, we confirmed that long-term storage at 4 °C also promoted crystal precipitation in the stock solutions of sUA (Figure S8).

To reveal the role of sUA-CD38 interaction in regulating inflammation and innate immunity, at first, we stimulated WT and CD38 KO mice with crude lipopolysaccharide (cLPS) after 1-day sUA supplementation. OA was used as the background in mice to exclude its interference. Plasma sUA at the minimum physiological levels of humans (OA plus inosine groups) suppressed cLPS-induced production of serum IL-1β and IL-18 in WT mice without affecting inflammasome-independent TNF-α levels, and the suppressive effects were abrogated in CD38 KO mice (Figures 4A-4C), demonstrating that sUA physiologically limits cLPS-induced systemic inflammation via CD38. sUA immunosuppression may be partially mediated by increased NAD^+ levels and decreased cADPR production in whole blood after sUA-CD38 interaction (Figures S3D and S3F). sUA hardly limited high-dose cLPS-induced systemic inflammation (Figures S5A-S5C), although plasma sUA and whole blood NAD^+ levels were increased (Figures S5D and S5E). In addition, high-dose cLPS, with or without sUA supplementation, did not affect cADPR levels (Figure S5G), suggesting some CD38-independent inflammatory mechanisms.

Recently, crystal-free hyperuricemia has been shown to rapidly inhibit neutrophil migration (46), suggesting that some biological targets directly mediate sUA immunosuppression (47). CD38 is crucial for neutrophil recruitment (27), we therefore investigated the effect of sUA on MSU crystal-induced peritonitis via CD38. After 1-day sUA supplementation, plasma sUA at the minimum physiological levels of humans (OA plus inosine groups) inhibited the recruitment of viable cells and neutrophils and reduced the production of IL-1β and IL-6 in WT mice but not in CD38 KO mice (Figures 4D, 4E, 4G, and 4H), which verified the involvement of CD38 in the suppressive effect of sUA on inflammation and innate immunity. CXCL1 production (Figure 4F) was not affected by sUA, indicating that the sUA-CD38 interaction may

inhibit circulating immune cells in response to chemokines. Moreover, sUA may interfere with the interaction between CD38 and adhesion molecules such as CD31(48, 49) to suppress immune cell migration. Intriguingly, intact IL-8 signaling has been reported in CD38 KO mice (27), and sUA at a high concentration (595 μM) inhibits neutrophils in response to IL-8 (46). Whereas we did not observe decreased neutrophil recruitment by sUA in CD38 KO mice, likely because plasma sUA levels (around 120 μM) in our models are insufficient to affect IL-8 signaling. In addition, we cannot exclude the possibility that CD38 is essential for the inhibitory effects of sUA on IL-8 signaling and β2-integrin, which requires further investigation in the future.

Inosine, an sUA precursor, may also exhibit anti-inflammatory effect by interacting with adenosine receptors (50). Scott, et al. reported that after oral administration, serum inosine concentrations slightly increased and then rapidly returned to the initial levels in mice within 2 h (8). We stimulated the mice with cLPS or MSU crystals 2 h after the second treatment, suggesting the negligible contribution of inosine. To verify this and exclude the potential contribution of OA, we evaluated the effects of 1-day treatment of inosine or OA on inflammation *in vivo*. The results showed that OA or inosine alone hardly affected cLPS-induced systemic inflammation (Figures S7B-S7D) and MSU crystal-induced peritonitis (Figures S7E-S7I), as well as plasma sUA levels and whole blood NAD^+ metabolism under inflammatory conditions (Figures S3G-S3J). Thus, these results suggested that sUA at physiological levels limits innate immunity to avoid excessive inflammation by interacting with CD38.

Discussion

In the present study, we unveiled CD38 as a direct physiological target for sUA and thus defined its fundamental physiological functions in the regulation of NAD^+ availability and innate immunity, which promotes understanding of the molecular basis of sUA physiology as well as providing an important clue to explore the potential impact of abnormal sUA levels (independent of MSU crystals) on health and disease.

It has been reported that NAD^+ decline contributes to inflammation, aging-related dysfunction, and multiple diseases, including hearing loss, obesity, diabetes, kidney diseases, and cardiovascular diseases, in murine models (21) and possibly even in humans (51). Accordingly, NAD^+ boosting by CD38 inhibitors has been a promising therapeutic strategy (21, 23, 52). We discovered a structural feature for pharmacological inhibition of CD38 based on sUA analogs such as caffeine metabolites, which may facilitate the development of new inhibitors with ideal pharmacokinetic properties because sUA is rarely metabolized and is well distributed in humans, although chemical modification is required to improve inhibitory efficiency and specificity. Indeed, sUA and its analogs have similar functions, such as antioxidant property (53) and neuroprotective effects (54), supporting that they share a functional group, 1,3-dihydroimidazol-2-one, that interacts with the same targets, including but not limited to CD38. Importantly, our results support that sUA at physiological levels limits CD38 activity to maintain NAD^+ availability, providing the molecular basis for sUA preventing NAD^+ decline-associated diseases and senescence. The apparent K_i values imply that CD38 is completely inhibited by sUA in blood or in some tissues under physiological conditions; however, this might not be the case because other endogenous substance may also regulate CD38 activity (55-57). In spite of this, altered sUA levels are able to indicate the changes in the activities of CD38 and other molecular targets of sUA, which partially explains the correlation between sUA homeostasis disruption and disease risk. For instance, abnormal reduction of sUA levels such as hypouricemia may result in higher CD38 activity in the circulation due to the reversible inhibitory effect of sUA, thus negatively influencing health as well as increasing the risk of certain diseases. However, it does not mean that higher sUA levels are better, because excessive elevation of sUA levels promotes the precipitation of MSU crystals. In addition, we cannot exclude the possibility that long-term and crystal-free hyperuricemia (> 420 μM) in humans may overly modulate additional unknown targets, especially in CD38-negative cells, thereby partially covering the CD38-mediated physiological functions of sUA. To identify more molecular targets for sUA, drug affinity responsive target stability (DARTS) (58) and cellular thermal shift assay (CETSA) (59), which detect the

direct responses of binding proteins to their ligands, may serve as alternative strategies.

Another unexpected observation is the restrictive effect of sUA at physiological levels on excessive inflammation, which is complementary to several recent studies regarding the immunosuppressive effect of crystal-free hyperuricemia in the host (45, 46). Similar to itaconate, an inhibitor of the NLRP3 inflammasome (60), sUA production increases in activated macrophages (61). It has been reported that intracellular sUA reduction promotes certain inflammatory responses (13, 61), hence sUA at physiological levels may function as an endogenous regulator of inflammasomes to avoid excessive inflammation by regulating CD38 activity. On the other hand, chemical phase transition (crystal precipitation) is essential for sUA as a danger signal to trigger immune responses (14, 44-46, 61, 62). We and another laboratory have demonstrated that CD38 activation by MSU crystals promotes gouty inflammation in primed macrophages (63, 64). Importantly, in this study, we showed that CD38 mediates the opposite effects of sUA (even at physiological levels) and MSU crystals on inflammation and innate immunity. Therefore, a sudden and rapid reduction of the circulating sUA levels by high-dose urate-lowering medications may disrupt the immune balance by rapidly releasing CD38 activity before MSU crystal dissolution (Figure S9), resulting in the increased gout attacks in patients (12), a well-known paradox in gout therapy. Several clinical studies even observed that blood sUA levels decrease during gout flares, while the resolution of gouty inflammation is coming with a recovery of sUA levels (65, 66). Given the distinct effects of sUA and MSU crystals on certain targets, intracellular and/or extracellular microcrystals should be excluded when evaluating the pathological role of sUA at high levels in relevant studies. In addition, our findings also provide biological evidence for the neuroprotection of sUA. It has been reported that CD38 is involved in neurodegenerative diseases (67, 68), thus, sUA in central nervous system (CNS) tissues may directly inhibit CD38 activity to limit neuroinflammation and the progression of such diseases.

Previously, a physiological medium containing sUA was shown to inhibit UMP

synthase to reshape cellular metabolism *in vitro* (69). We identified a unique sUA-CD38 interaction in this study, highlighting the physiologically essential role of sUA as a purine metabolite in sustaining life. Accumulated data suggest a remarkable overlap between the effects of sUA (8-10, 15-20, 45, 46) and CD38 inhibition/KO (21, 23, 67, 68) in counteracting inflammation, aging, and certain diseases, which also strongly supports our current findings. It should be noticed that we used an exogenous compound as the background in mice to mimic the deficiency of uricase in humans, and tissue sUA levels were unchanged after sUA supplementation, suggesting some of the limitations in our models when evaluating the physiological relevance. Therefore, it is important to extend these studies to global sUA-depletion models in primates or uricase-transgenic mice. Moreover, the commercial recombinant hCD38 without a transmembrane region was partially used in this study, we cannot exclude the potential interaction between sUA and the transmembrane region of CD38, although comparable K_i values were obtained in crude enzymes containing full-length CD38. In addition to identification of the allosteric sites of CD38, the crystal structure of the active full-length CD38-sUA complex should be also captured using cryo-electron microscopy to elucidate the inhibitory mechanisms in the future. However, the present study clearly demonstrated that sUA at physiological levels directly inhibits CD38 and consequently limits NAD^+ degradation and excessive inflammation, suggesting that sUA is crucial for the physiological defense in humans against aging and diseases.

Materials and methods

Materials and reagents used in this study are described in Table S1.

Animals

Male and female ICR (Institute of Cancer Research of the Charles River Laboratories, Inc., Wilmington, MA, USA) mice were initially purchased from Japan SLC, Inc. CD38 KO mice (ICR strain) were generated using the CRISPR/Cas9 method as previously described (70). WT and CD38 KO mice were kept and bred at the Experimental Animal Center of Kanazawa University (Takara-machi campus). For animal experiments, all

the mice (sex and age as indicated in respective figure legends) were transferred a week in advance and housed in the animal room of Research Center of Child Mental Development under standard conditions (24 °C; 12 h light/dark cycle, lights on at 8:30 am) with standard chow and water provided *ad libitum*. Male and female mice were separated after weaning and were equally used for experiments except when specified. In each experimental group, the mice were from different biological mothers. All animal experiments were approved by the Institutional Animal Care and Use Committee at Kanazawa University (AP-214243), and were performed in accordance with ARRIVE and the local guidelines.

Cell culture

THP-1 and A549 cells were cultured in RPMI-1640 containing 10% FBS and 1% penicillin/streptomycin. Bone marrow cells and bone marrow-derived macrophages were maintained in RPMI-1640 containing 10% FBS, 1% penicillin/streptomycin, and 50 μM 2-mercaptoethanol in the presence or absence of macrophage colony stimulating factor (M-CSF).

Measurement of CD38 activity

The hydrolase activity of CD38 was measured according to a previous report (71) with minor modifications. CD38 hydrolase activity was measured using 50 μM ε-NAD^+ as a substrate in hydrolase reaction buffer (250 mM sucrose, 40 mM Tris-HCl, pH 7.4). Briefly, cells or tissues were directly homogenized in blank reaction buffer on ice, and recombinant hCD38 was diluted in blank reaction buffer for subsequent assays. The tissue homogenates were centrifuged to collect the supernatant for enzyme assays. The loading volume of enzyme was 4 to 30 μL, the total volume of the reaction system was 3 mL. To detect enzyme inhibition, except when specified, the ligands were directly dissolved in hydrolase reaction buffer before pH adjustment, after which, the pH was immediately adjusted to 7.4. All reaction buffers, with or without ligands, were freshly prepared before each assay. For measurement of hydrolase activity, 3 mL reaction buffer containing enzyme, ε-NAD^+, and ligands at indicated concentrations was maintained at

37 °C with constant stirring.

The cyclase activity of CD38 was measured as previously described (26, 72). CD38 cyclase activity was measured using 60 μM NGD as a substrate in cyclase reaction buffer (100 mM KCl, 10 μM $CaCl_2$ and 50 mM Tris-HCl, pH 6.6). Tissues were cut into pieces and suspended in lysis buffer (5 mM $MgCl_2$, 10 mM Tris-HCl, pH 7.3) at 4 °C for 30 min. Then, the suspension was homogenized on ice, and the supernatant was collected after centrifugation. To collect the crude membrane fractions, the supernatant was centrifuged at 105000 g for 30 min. The final pellet was resuspended in 10 mM Tris-HCl solution (pH 6.6) for cyclase assay. Homogenates of THP-1 or A549 cells, and recombinant hCD38 were used directly for cyclase assays. The loading volume of enzyme was 4 to 20 μL, the total volume of reaction system was 3 mL. To detect enzyme inhibition, except when specified, the ligands were directly dissolved in cyclase reaction buffer before pH adjustment, after which, the pH was immediately adjusted to 6.6. All reaction buffers, with or without ligands, were freshly prepared before each assay. For measurement of cyclase activity, 3 mL reaction buffer containing enzyme, NGD and ligands at indicated concentrations was maintained at 37 °C with constant stirring.

The reaction buffer for hydrolase or cyclase assays was excited at 300 nm, and fluorescence emission was measured every second at 410 nm by Shimazu RF-6000 spectrofluorometer. Hydrolase or cyclase activity was calculated from the linear portion of the time course by fitting a linear function to the data points recorded within 5 min.

In this study, 8-OG and guanosine were tested only at 50 μM due to the limited solubility. Guanosine was dissolved in DMSO and diluted in the reaction buffer for subsequent assays. Other ligands such as sUA, inosine, hypoxanthine, xanthine, allantoin, adenosine, uracil, 1,3-DHI-2-one, oxypurinol, caffeine, 1-MU, and 1,3-DMU were tested at 5 or 500 μM.

For reversibility test, recombinant hCD38 was pre-incubated for 30 min in 4 conditions: (1) control reaction buffer; (2) in the presence of 100 μM substrate (ε-NAD^+ or NGD); (3) 500 μM sUA; (4) both substrate and sUA. Subsequently, the enzyme was diluted 100-fold in reaction buffer in the presence or absence of 500 μM sUA for activity assays using ε-NAD^+ or NGD. Naïve THP-1 and A549 cells were incubated with RPMI-1640 medium in the presence or absence of 500 μM sUA for 2 h. The cells were collected and homogenized in the reaction buffer on ice with or without 500 μM sUA, samples were then diluted 100-fold in reaction buffer with or without 500 μM sUA for enzyme assay. Control group was not treated with sUA in all steps; sUA group was treated with sUA in each step; sUA release group was treated with sUA prior to dilution in sUA-free buffer for enzyme assays.

Moderate sUA supplementation in mice

Plasma sUA levels in mice were increased to the minimum physiological levels of humans by moderate sUA supplementation. For 1-day sUA supplementation, WT and CD38 KO mice received oral administration of saline, OA (1.5 g/kg), or OA (1.5 g/kg) plus inosine (1.5 g/kg), the gavage volume was 5 mL/kg. Drug suspension in saline was freshly prepared and warmed to 37 °C before each treatment. The mice received the first treatment on the evening (19:00) of the first day and the second treatment on the morning (9:00) of the second day. For 3-day or 7-day sUA supplementation, WT and CD38 KO mice received the same treatment twice daily from the evening of the first day to the morning of the last day. Four hours after the last treatment, the mice were sacrificed and whole blood, serum, plasma, and tissues were collected for metabolic studies. For immunological studies, mice were stimulated with different ligands 2 h after the second treatment on the morning (9:00) of the second day.

sUA release in mice

WT mice received oral administration of saline, OA, or OA plus inosine (1-day supplementation model, as described above). One day (28 h) or 3 days (76 h) after the second treatment, the mice were sacrificed and whole blood and plasma were collected.

cLPS-induced systemic inflammation

Plasma sUA levels in WT and CD38 KO mice were increased to the minimum physiological levels of humans by 1-day sUA supplementation (OA plus inosine). Two hours after the last treatment of OA, or OA plus inosine, the mice were intraperitoneally injected with sterile PBS or cLPS (2 mg/kg or 20 mg/kg), the injection volume was 3 mL/kg. Four hours (20 mg/kg) or 6 h (2 mg/kg) after stimulation, the mice were sacrificed and whole blood, plasma, and serum were collected.

MSU crystal-induced peritonitis

Plasma sUA levels in WT and CD38 KO mice were increased to the minimum physiological levels of humans by 1-day sUA supplementation (OA plus inosine). Two hours after the last treatment of OA, or OA plus inosine, the mice were intraperitoneally injected with sterile PBS or MSU crystals (2 mg/mouse), and the injection volume was 200 μL/mouse. Six hours after stimulation, the mice were sacrificed and blood samples were collected. For each mouse, the peritoneal cavity was washed with 5 mL ice-cold sterile PBS, the supernatant was collected by centrifugation for subsequent ELISA, and cell pellets were used for total viable cell count by Trypan Blue staining and neutrophil count by Wright-Giemsa staining. In brief, cell pellet from 1.5 mL of peritoneal lavage fluid was resuspended in RBC lysis buffer for 30 s, PBS (9-fold volume) was added to terminate lysis. Afterward, the cells were centrifuged at 1000 rpm for 5 min and resuspended in PBS for viable cell count. For neutrophil count, peritoneal lavage fluid was directly used for smears after appropriate dilution, and subsequently, Wright-Giemsa staining was performed according to the protocol provided by the manufacturer. Viable cells and neutrophils were counted by two investigators, and the mean numbers were shown in the figures.

ELISA

Human IL-1β, mouse IL-1β, IL-6, IL-18, TNFα and CXCL1 levels were measured according to the protocols provided by the manufacturer. Serum samples were diluted

before ELISA when applicable. In this study, all the samples were frozen after collection and thawed before ELISA.

Preparation of MSU crystal and sUA solution

MSU crystals were prepared by the recrystallization of oversaturated sUA according to a previous report (5). Improper preparation of sUA solution may introduce crystals to cause false-positive or false-negative results. It has been demonstrated that crystals may precipitate in sUA solution prepared by pre-warming to activate immune cells (45). In this study, the sUA solution was prepared according to an improved protocol (45). Briefly, we directly dissolved sUA at 0.5 mg/mL in blank RPMI-1640 medium by addition of NaOH, and adjusted the pH by HCl. Then sUA solution was immediately filtered by 0.2-μm filters and diluted to experimental concentration (up to 10 mg/L, 595 μM). For all experiments, sUA solution was freshly prepared and used immediately.

Preparation of BMDMs

BMDMs were prepared and primed as previously described (63). In brief, bone marrow cells were isolated from 10- to 12-week-old WT or CD38 KO mice by washing the marrow cavity with sterile PBS. The collected bone marrow cells were filtered by 70-μm strainers and then centrifuged at 1000 rpm, 4°C for 5 min. The cell pellet was resuspended in 2 mL red blood cell (RBC) lysis buffer for 30 s, then 8 mL complete RPMI-1640 medium (10% FBS, 1% Penicillin/Streptomycin and 50 μM 2-mercaptoethanol) was added to terminate the lysis. After 5-min centrifugation at 1000 rpm, 4°C, the cells were resuspended in fresh complete RPMI-1640 medium and maintained for 4 h in an incubator. Adherent cells were discarded, whereas non-adherent cells were cultured in complete RPMI-1640 medium containing 20 ng/mL M-CSF. After 3-day differentiation, the medium was replaced with fresh complete RPMI-1640 medium containing 20 ng/mL M-CSF. On the 7th day, BMDMs were collected for subsequent experiments. BMDMs were primed with 100 ng/mL ultrapure LPS for 4 h for canonical inflammasome assay. For metabolic assay of NMN, BMDMs were primed with 100 ng/mL ultrapure LPS for 8 h to induce higher protein expression of CD38.

Intracellular NAD^+ assay

A549 cells were seeded in 24-well plates for NAD^+ assay. Briefly, when the confluence reached 80%, the culture medium in each well was discarded, and the cells were washed twice with PBS and incubated in RPMI-1640 medium containing 1% FBS in the presence or absence of sUA (from 100 to 500 μM) for 20 h. Then the cells were washed twice with PBS, after the second washing, PBS was completely removed and 100 μL 5% ice-cold PCA was added into each well. The plate was kept on ice for 2 h, then cell samples were collected and centrifuged at 15000 rpm, 4°C for 10 min. The supernatant was used for subsequent handling and measurement (see LC-MS/MS analysis).

Naïve THP-1 cells were pre-incubated with sUA (0-10 mg/dL) in RPMI-1640 medium containing 1% FBS for 2h, then the cells were washed twice with PBS and stimulated with MSU crystals, cLPS, zymosan or ATP for 6 h. Subsequently, the cells were washed twice with PBS, and then a total of 100 μL 5% ice-cold PCA was used to extract NAD^+ from cells in each well and medium as mentioned above.

WT BMDMs were primed with 100 ng/mL ultrapure LPS for 8 h. Then the cells were washed twice with PBS. Afterward, the cells were incubated in control or 100 μM NMN-supplemented RPMI-1640 medium in the presence of sUA or 78c. After 6-h incubation, the cells were washed twice with PBS. Finally, cell samples for NAD^+ measurement were collected by 5% ice-cold PCA as mentioned above.

Canonical inflammasome assay

Naïve THP-1 cells were primed with 0.5 μM phorbol 12-myristate 13-acetate (PMA) for 3 h the day before stimulation. Primed THP-1 cells were pre-incubated in RPMI-1640 medium in the presence or absence of sUA (5 or 10 mg/dL) for 2 h. The cells were then washed twice with PBS, and were stimulated with MSU crystals, cLPS, zymosan, and ATP in serum-free RPMI-1640 medium for 4 h.

WT and CD38 KO BMDMs were primed with 100 ng/mL ultrapure LPS for 4 h. Subsequently, primed BMDMs were pre-incubated with or without sUA (5 or 10 mg/dL) for 2 h, the cells were then washed twice with PBS and were stimulated with nigericin, MSU crystals, or cLPS in serum-free RPMI-1640 medium.

After stimulation, the culture medium was collected and centrifuged at 3000 rpm, 4 ℃ for 5 min, the supernatant was collected and stored at -30 ℃ until ELISA.

sUA uptake assay

WT BMDMs were primed with 100 ng/mL ultrapure LPS for 4 h. Then the cells were washed twice with PBS, and maintained in RPMI-1640 medium containing sUA (100, 200, or 500 μM) for 2 h or 15 h. Subsequently, the cells were washed twice with ice-cold PBS to terminate uptake, 100 μL 5% ice-cold PCA was added into each well. The plates were placed on ice for 2 h, then cell samples were collected and centrifuged at 15000 rpm, 4℃ for 10 min. The supernatant was used for subsequent handling and measurement (see LC-MS/MS analysis).

Metabolic assay of NAD^+

NAD^+ degradation by recombinant hCD38 was detected in hydrolase reaction buffer. At first, sUA (100, 200 and 500 μM) or other ligands at 500 μM in hydrolase reaction buffer (250 mM sucrose, 40 mM Tris) was freshly prepared, then the pH was immediately adjusted to 7.4 by HCl. Recombinant hCD38 was added into the buffer of experimental groups at 20 ng/mL, then the buffer was maintained at 37 ℃. The substrate NAD^+ was dissolved in hydrolase reaction buffer (pH 7.4) at 10 mM, and the pH was further adjusted to 7.4. The reaction was started with the addition of NAD^+ in the buffer for each group (final concentration is 200 μM), including control group (recombinant hCD38 free). All the buffers were incubated at 37 ℃ with constant stirring. After 30 or 60 min, 20 μL reaction buffer was transferred into 180 μL of 5% ice-cold PCA, then vortexed for 30 s before 10-min centrifugation at 15000 rpm, 4 ℃. The supernatant was further handled for NAD^+ measurement within 12 h without

freezing and thawing (see LC-MS/MS analysis).

Metabolic assay of NMN

To prepare the reaction buffer, sUA was directly dissolved in blank RPMI-1640 medium by addition of NaOH, and the pH was immediately adjusted by HCl. After pH adjustment, the medium containing sUA was filtered by 0.2-μm filter and diluted as indicated. The medium containing 20 ng/mL recombinant hCD38 was then placed in a cell incubator. The reaction was started with the addition of NMN (final concentration was 200 μM). After incubation for 6 h, 20 μL medium was transferred into 180 μL 5% ice-cold PCA, then vortexed for 30 s and centrifuged at 15000 rpm, 4 °C for 10 min. The supernatant was stored at -80 °C until further handling for NMN measurement (see LC-MS/MS analysis).

Extracellular NMN degradation

WT and CD38 KO BMDMs were primed with 100 ng/mL ultrapure LPS for 8 h, then the cells were washed twice with PBS. Primed BMDMs were maintained in RPMI-1640 medium supplemented with 100 μM NMN in the presence or absence of sUA. To restore the inhibitory effects of sUA on NMN degradation in KO BMDMs, recombinant hCD38 was added to the medium (final concentration was 10 ng/mL). After 6-h incubation, culture medium was collected and centrifuged at 3000 rpm, 4 °C for 5 min. Then, 20 μL of supernatant was transferred into 180 μL 5% ice-cold PCA, and was vortexed for 30 s and centrifuged at 15000 rpm, 4 °C for 10 min. The supernatant was stored at -80 °C until further handling for NMN measurement.

Handling of animal samples

The collected whole blood samples were immediately diluted 10-fold in 5% ice-cold perchloric acid (PCA) and homogenized on ice. After 10-min centrifugation at 15000 rpm, 4 °C, the supernatant was subpackaged for measurement or -80 °C storage. For NAD^+ measurement in whole blood, the supernatant was handled without freezing and thawing and was measured within 24 h of sample collection. For measurement of

plasma sUA, after sample collection, we immediately diluted the plasma with 5% ice-cold PCA, after vortex, samples were centrifuged at 15000 rpm, 4 °C for 10 min, the collected supernatant was used for the subsequent handling and measurement within 24 h.

After the collection of blood samples, the mice were immediately perfused with ice-cold PBS. The tissue samples were collected, dried with tissue paper, and weighed. All the tissue samples were immediately homogenized in 5% ice-cold PCA on ice, then centrifuged at 15000 rpm, 4°C for 10 min. The supernatant was collected and stored at -80 °C until further handling for measurement (see LC-MS/MS analysis).

LC-MS/MS analysis

As mentioned above, samples (cells, tissues, blood or reaction buffer) were treated with ice-cold PCA, after extraction and centrifugation, the collected supernatant was appropriately diluted in 5% ice-cold PCA, and then was vortexed for 30 s and centrifuged at 15000 rpm, 4°C for 5 min. Afterward, 30 μL supernatant was added into 200 μL 5 mM ammonium formate containing internal standards at indicated concentrations. Then all the samples were vortexed for 30 s and centrifuged at 15000 rpm, 4°C for 5 min again, the final supernatant was used for subsequent measurement. All the samples after handling were immediately analyzed in this study without freezing and thawing.

The LC-MS/MS system consisted of a triple quadrupole LCMS-8050 (Shimadzu) and an LC-30A system (Shimadzu). NAD^+, NMN and the N-cyclohexyl benzamide (NCB, internal standard, 5 ng/mL) were eluted on Altlantis® HILIC Silica (2.1 × 150 mm, 5 μm) at 40 °C using an isocratic mobile phase containing 60% water with 0.1% formic acid and 40% acetonitrile with 0.1% formic acid at 0.4 mL/min. The selected transitions of m/z were 664.10 → 136.10 for NAD^+, 334.95 → 123.15 for NMN, and 204.10 → 122.20 for NCB in positive ion mode. NAD^+ and NMN were measured independently in this study, as their peaks were hardly separated within a short time.

sUA, cADPR and FYU-981 (internal standard, 1 μM, Fuji Yakuhin Co., Ltd.) were eluted on CAPCELL PAK C8 TYPE UG 120 (2 × 150 mm, 5 μm) at 40 °C. sUA and FYU-981 were separated using a gradient mobile phase containing water with 0.1% formic acid (A) and acetonitrile with 0.1% formic acid (B) at 0.4 mL/min. The elution was started with 55% A for 0.5 min, A was decreased from 55% to 5% for 1 min, then A was increased from 5% to 55% for 0.5 min, finally 55% A was maintained for 0.5 min. cADPR and FYU-981 were separated using an isocratic mobile phase containing 60% water with 0.1% formic acid and 40% acetonitrile with 0.1% formic acid at 0.4 mL/min. The selected transitions of m/z were 167.10 → 124.10 for sUA, 539.95 → 272.95 for cADPR, and 355.95 → 159.90 for FYU-981 in negative ion mode.

The injection volume was 1 μL for all measurements, and data manipulation was accomplished by Labsolutions software (version 5.97, Shimadzu).

Statistical analysis

Statistics were performed using GraphPad Prism 9. Sample size was not predetermined by any statistical methods. Comparisons between multiple groups were performed using 1-way ANOVA with Dunnett's or Tukey's multiple comparisons test or 2-way ANOVA with Tukey's multiple comparisons test when applicable. Two-tailed unpaired t-test or Mann-Whitney test were used for the analysis between two groups when applicable. The normality test was performed using GraphPad Prism 9 before parametric statistical analysis. Data were shown as mean ± s.e.m. or mean ± s.d. as indicated. $p < 0.05$ was considered significant. The details of statistical tests and the numbers of mice or biologically independent samples were described in the figure legends.

Author contributions

S.W. and I.T. designed the study. S.W. performed experiments and wrote the manuscript. S.W., H.A., and I.T. analyzed the data. H.A. provided support in the whole project. S.W.,

H.A., H.H, and I.T. edited the manuscript. All the authors discussed the results and reviewed and approved the manuscript. H.A., S.Y., Y.S., and H.H. provided animals, and/or a part of materials and instruments. H.A., S.Y., and H.H. assisted with experimental design. H.H. advised enzyme assay. I.T. was the leader of whole project and supervised this study.

Acknowledgments

This study was supported by KAKENHI [JP21H02641] (I.T.), [JP23K18181] (I.T.), and [JP22K19372] (H.A.) from the Japan Society for the Promotion of Science (JSPS) and Research Grant 2022 (I.T.) from Gout and Uric Acid Foundation of Japan. S.W. was funded by the Japanese Government (Monbukagakusho: MEXT) Scholarship Program and Kanazawa University. The authors thank Dr. Zheng Jing, Ms. Aimi Taniguchi, Mr. Kazuki Himi, and Mr. Kazuki Fujita for providing assistance.

Data availability

All data generated or analyzed in this study are provided in the article and supplemental information.

Conflict of interest

The authors declare no competing interests.

References

1. Oda M, Satta Y, Takenaka O, Takahata N. Loss of urate oxidase activity in hominoids and its evolutionary implications. Mol Biol Evol. 2002;19(5):640-53.

2. Wu XW, Muzny DM, Lee CC, Caskey CT. Two independent mutational events in the loss of urate oxidase during hominoid evolution. J Mol Evol. 1992;34(1):78-84.

3. Glantzounis GK, Tsimoyiannis EC, Kappas AM, Galaris DA. Uric acid and oxidative stress. Curr Pharm Des. 2005;11(32):4145-51.

4. Watanabe S, Kang DH, Feng L, Nakagawa T, Kanellis J, Lan H, et al. Uric acid, hominoid evolution, and the pathogenesis of salt-sensitivity. Hypertension.

2002;40(3):355-60.

5. Martinon F, Pétrilli V, Mayor A, Tardivel A, Tschopp J. Gout-associated uric acid crystals activate the NALP3 inflammasome. Nature. 2006;440(7081):237-41.

6. Dehlin M, Jacobsson L, Roddy E. Global epidemiology of gout: prevalence, incidence, treatment patterns and risk factors. Nat Rev Rheumatol. 2020;16(7):380-90.

7. Howles SA, Thakker RV. Genetics of kidney stone disease. Nat Rev Urol. 2020;17(7):407-21.

8. Scott GS, Spitsin SV, Kean RB, Mikheeva T, Koprowski H, Hooper DC. Therapeutic intervention in experimental allergic encephalomyelitis by administration of uric acid precursors. Proc Natl Acad Sci U S A. 2002;99(25):16303-8.

9. Kutzing MK, Firestein BL. Altered uric acid levels and disease states. J Pharmacol Exp Ther. 2008;324(1):1-7.

10. Lu N, Dubreuil M, Zhang Y, Neogi T, Rai SK, Ascherio A, et al. Gout and the risk of Alzheimer's disease: a population-based, BMI-matched cohort study. Ann Rheum Dis. 2016;75(3):547-51.

11. Crawley WT, Jungels CG, Stenmark KR, Fini MA. U-shaped association of uric acid to overall-cause mortality and its impact on clinical management of hyperuricemia. Redox Biol. 2022;51:102271.

12. Becker MA, Schumacher HR, Jr., Wortmann RL, MacDonald PA, Eustace D, Palo WA, et al. Febuxostat compared with allopurinol in patients with hyperuricemia and gout. N Engl J Med. 2005;353(23):2450-61.

13. Kono H, Chen CJ, Ontiveros F, Rock KL. Uric acid promotes an acute inflammatory response to sterile cell death in mice. J Clin Invest. 2010;120(6):1939-49.

14. Shi Y. Caught red-handed: uric acid is an agent of inflammation. J Clin Invest. 2010;120(6):1809-11.

15. Álvarez-Lario B, Macarrón-Vicente J. Uric acid and evolution. Rheumatology. 2010;49(11):2010-5.

16. Ames BN, Cathcart R, Schwiers E, Hochstein P. Uric acid provides an antioxidant defense in humans against oxidant- and radical-caused aging and cancer: a hypothesis. Proc Natl Acad Sci U S A. 1981;78(11):6858-62.

17. Cutler RG, Camandola S, Feldman NH, Yoon JS, Haran JB, Arguelles S, et al. Uric acid enhances longevity and endurance and protects the brain against ischemia. Neurobiol Aging. 2019;75:159-68.

18. Wan QL, Fu X, Dai W, Yang J, Luo Z, Meng X, et al. Uric acid induces stress resistance and extends the life span through activating the stress response factor DAF-16/FOXO and SKN-1/NRF2. Aging. 2020;12(3):2840-56.

19. Lai JH, Luo SF, Hung LF, Huang CY, Lien SB, Lin LC, et al. Physiological concentrations of soluble uric acid are chondroprotective and anti-inflammatory. Sci Rep. 2017;7(1):2359.

20. Linnerz T, Sung YJ, Rolland L, Astin JW, Dalbeth N, Hall CJ. Uricase-Deficient Larval Zebrafish with Elevated Urate Levels Demonstrate Suppressed Acute Inflammatory Response to Monosodium Urate Crystals and Prolonged Crystal Persistence. Genes. 2022;13(12):2179.

21. Hogan KA, Chini CCS, Chini EN. The Multi-faceted Ecto-enzyme CD38: Roles in Immunomodulation, Cancer, Aging, and Metabolic Diseases. Front Immunol. 2019;10:1187.

22. Luongo TS, Eller JM, Lu MJ, Niere M, Raith F, Perry C, et al. SLC25A51 is a mammalian mitochondrial NAD(+) transporter. Nature. 2020;588(7836):174-9.

23. Chini EN, Chini CCS, Espindola Netto JM, de Oliveira GC, van Schooten W. The Pharmacology of CD38/NADase: An Emerging Target in Cancer and Diseases of Aging. Trends Pharmacol Sci. 2018;39(4):424-36.

24. Lee HC. Physiological functions of cyclic ADP-ribose and NAADP as calcium messengers. Annu Rev Pharmacol Toxicol. 2001;41:317-45.

25. Lee HC, Walseth TF, Bratt GT, Hayes RN, Clapper DL. Structural determination of a cyclic metabolite of NAD+ with intracellular Ca2+-mobilizing activity. J Biol Chem. 1989;264(3):1608-15.

26. Jin D, Liu HX, Hirai H, Torashima T, Nagai T, Lopatina O, et al. CD38 is critical for social behaviour by regulating oxytocin secretion. Nature. 2007;446(7131):41-5.

27. Partida-Sánchez S, Cockayne DA, Monard S, Jacobson EL, Oppenheimer N, Garvy B, et al. Cyclic ADP-ribose production by CD38 regulates intracellular calcium

release, extracellular calcium influx and chemotaxis in neutrophils and is required for bacterial clearance in vivo. Nat Med. 2001;7(11):1209-16.

28. Kuwabara M, Niwa K, Ohtahara A, Hamada T, Miyazaki S, Mizuta E, et al. Prevalence and complications of hypouricemia in a general population: A large-scale cross-sectional study in Japan. PloS one. 2017;12(4):e0176055.

29. Dalbeth N, Gosling AL, Gaffo A, Abhishek A. Gout. Lancet. 2021;397(10287):1843-55.

30. Traut TW. Physiological concentrations of purines and pyrimidines. Mol Cell Biochem. 1994;140(1):1-22.

31. Eells JT, Spector R. Purine and pyrimidine base and nucleoside concentrations in human cerebrospinal fluid and plasma. Neurochem Res. 1983;8(11):1451-7.

32. Dudzinska W, Lubkowska A, Dolegowska B, Safranow K, Jakubowska K. Adenine, guanine and pyridine nucleotides in blood during physical exercise and restitution in healthy subjects. Eur J Appl Physiol. 2010;110(6):1155-62.

33. Chini CCS, Peclat TR, Warner GM, Kashyap S, Espindola-Netto JM, de Oliveira GC, et al. CD38 ecto-enzyme in immune cells is induced during aging and regulates NAD(+) and NMN levels. Nat Metab. 2020;2(11):1284-304.

34. Fridovich I. THE COMPETITIVE INHIBITION OF URICASE BY OXONATE AND BY RELATED DERIVATIVES OF S-TRIAZINES. J Biol Chem. 1965;240:2491-4.

35. Mills KF, Yoshida S, Stein LR, Grozio A, Kubota S, Sasaki Y, et al. Long-Term Administration of Nicotinamide Mononucleotide Mitigates Age-Associated Physiological Decline in Mice. Cell Metab. 2016;24(6):795-806.

36. Camacho-Pereira J, Tarragó MG, Chini CCS, Nin V, Escande C, Warner GM, et al. CD38 Dictates Age-Related NAD Decline and Mitochondrial Dysfunction through an SIRT3-Dependent Mechanism. Cell Metab. 2016;23(6):1127-39.

37. Minhas PS, Liu L, Moon PK, Joshi AU, Dove C, Mhatre S, et al. Macrophage de novo NAD(+) synthesis specifies immune function in aging and inflammation. Nat Immunol. 2019;20(1):50-63.

38. Misawa T, Takahama M, Kozaki T, Lee H, Zou J, Saitoh T, et al. Microtubule-

driven spatial arrangement of mitochondria promotes activation of the NLRP3 inflammasome. Nat Immunol. 2013;14(5):454-60.

39. He M, Chiang HH, Luo H, Zheng Z, Qiao Q, Wang L, et al. An Acetylation Switch of the NLRP3 Inflammasome Regulates Aging-Associated Chronic Inflammation and Insulin Resistance. Cell Metab. 2020;31(3):580-91.e5.

40. Murakami T, Ockinger J, Yu J, Byles V, McColl A, Hofer AM, et al. Critical role for calcium mobilization in activation of the NLRP3 inflammasome. Proc Natl Acad Sci U S A. 2012;109(28):11282-7.

41. Zeidler JD, Kashyap S, Hogan KA, Chini EN. Implications of the NADase CD38 in COVID pathophysiology. Physiol Rev. 2022;102(1):339-41.

42. Piedra-Quintero ZL, Wilson Z, Nava P, Guerau-de-Arellano M. CD38: An Immunomodulatory Molecule in Inflammation and Autoimmunity. Front Immunol. 2020;11:597959.

43. Joosten LAB, Crişan TO, Bjornstad P, Johnson RJ. Asymptomatic hyperuricaemia: a silent activator of the innate immune system. Nat Rev Rheumatol. 2020;16(2):75-86.

44. Alberts BM, Barber JS, Sacre SM, Davies KA, Ghezzi P, Mullen LM. Precipitation of Soluble Uric Acid Is Necessary for In Vitro Activation of the NLRP3 Inflammasome in Primary Human Monocytes. J Rheumatol. 2019;46(9):1141-50.

45. Ma Q, Honarpisheh M, Li C, Sellmayr M, Lindenmeyer M, Böhland C, et al. Soluble Uric Acid Is an Intrinsic Negative Regulator of Monocyte Activation in Monosodium Urate Crystal-Induced Tissue Inflammation. J Immunol. 2020;205(3):789-800.

46. Ma Q, Immler R, Pruenster M, Sellmayr M, Li C, von Brunn A, et al. Soluble uric acid inhibits β2 integrin-mediated neutrophil recruitment in innate immunity. Blood. 2022;139(23):3402-17.

47. Lowell CA. Hyperuricemia reduces neutrophil function. Blood. 2022;139(23):3354-6.

48. Deaglio S, Morra M, Mallone R, Ausiello CM, Prager E, Garbarino G, et al. Human CD38 (ADP-ribosyl cyclase) is a counter-receptor of CD31, an Ig superfamily member. J Immunol. 1998;160(1):395-402.

49. Deaglio S, Aydin S, Grand MM, Vaisitti T, Bergui L, D'Arena G, et al. CD38/CD31 interactions activate genetic pathways leading to proliferation and migration in chronic lymphocytic leukemia cells. Mol Med. 2010;16(3-4):87-91.

50. Gomez G, Sitkovsky MV. Differential requirement for A2a and A3 adenosine receptors for the protective effect of inosine in vivo. Blood. 2003;102(13):4472-8.

51. Rajman L, Chwalek K, Sinclair DA. Therapeutic Potential of NAD-Boosting Molecules: The In Vivo Evidence. Cell Metab. 2018;27(3):529-47.

52. Peclat TR, Shi B, Varga J, Chini EN. The NADase enzyme CD38: an emerging pharmacological target for systemic sclerosis, systemic lupus erythematosus and rheumatoid arthritis. Curr Opin Rheumatol. 2020;32(6):488-96.

53. Nishida Y. Inhibition of lipid peroxidation by methylated analogues of uric acid. J Pharm Pharmacol. 1991;43(12):885-7.

54. Haberman F, Tang SC, Arumugam TV, Hyun DH, Yu QS, Cutler RG, et al. Soluble neuroprotective antioxidant uric acid analogs ameliorate ischemic brain injury in mice. Neuromolecular Med. 2007;9(4):315-23.

55. Hara-Yokoyama M, Kukimoto I, Nishina H, Kontani K, Hirabayashi Y, Irie F, et al. Inhibition of NAD+ glycohydrolase and ADP-ribosyl cyclase activities of leukocyte cell surface antigen CD38 by gangliosides. J Biol Chem. 1996;271(22):12951-5.

56. Chini EN, de Toledo FG, Thompson MA, Dousa TP. Effect of estrogen upon cyclic ADP ribose metabolism: beta-estradiol stimulates ADP ribosyl cyclase in rat uterus. Proc Natl Acad Sci U S A. 1997;94(11):5872-6.

57. Dogan S, White TA, Deshpande DA, Murtaugh MP, Walseth TF, Kannan MS. Estrogen increases CD38 gene expression and leads to differential regulation of adenosine diphosphate (ADP)-ribosyl cyclase and cyclic ADP-ribose hydrolase activities in rat myometrium. Biol Reprod. 2002;66(3):596-602.

58. Lomenick B, Hao R, Jonai N, Chin RM, Aghajan M, Warburton S, et al. Target identification using drug affinity responsive target stability (DARTS). Proc Natl Acad Sci U S A. 2009;106(51):21984-9.

59. Martinez Molina D, Jafari R, Ignatushchenko M, Seki T, Larsson EA, Dan C, et al. Monitoring drug target engagement in cells and tissues using the cellular thermal shift

assay. Science. 2013;341(6141):84-7.
60. Hooftman A, Angiari S, Hester S, Corcoran SE, Runtsch MC, Ling C, et al. The Immunomodulatory Metabolite Itaconate Modifies NLRP3 and Inhibits Inflammasome Activation. Cell Metab. 2020;32(3):468-78.e7.
61. Ives A, Nomura J, Martinon F, Roger T, LeRoy D, Miner JN, et al. Xanthine oxidoreductase regulates macrophage IL1β secretion upon NLRP3 inflammasome activation. Nat Commun. 2015;6:6555.
62. Shi Y, Evans JE, Rock KL. Molecular identification of a danger signal that alerts the immune system to dying cells. Nature. 2003;425(6957):516-21.
63. Wen S, Arakawa H, Tamai I. CD38 activation by monosodium urate crystals contributes to inflammatory responses in human and murine macrophages. Biochem Biophys Res Commun. 2021;581:6-11.
64. Yan TC. CD38 Inhibition Attenuates Monosodium Urate Crystal-induced Inflammation in Macrophages. Dissertation, University of California, San Diego; 2021.
65. Logan JA, Morrison E, McGill PE. Serum uric acid in acute gout. Ann Rheum Dis. 1997;56(11):696-7.
66. Urano W, Yamanaka H, Tsutani H, Nakajima H, Matsuda Y, Taniguchi A, et al. The inflammatory process in the mechanism of decreased serum uric acid concentrations during acute gouty arthritis. J Rheumatol. 2002;29(9):1950-3.
67. Blacher E, Dadali T, Bespalko A, Haupenthal VJ, Grimm MO, Hartmann T, et al. Alzheimer's disease pathology is attenuated in a CD38-deficient mouse model. Ann Neurol. 2015;78(1):88-103.
68. Meyer T, Shimon D, Youssef S, Yankovitz G, Tessler A, Chernobylsky T, et al. NAD(+) metabolism drives astrocyte proinflammatory reprogramming in central nervous system autoimmunity. Proc Natl Acad Sci U S A. 2022;119(35):e2211310119.
69. Cantor JR, Abu-Remaileh M, Kanarek N, Freinkman E, Gao X, Louissaint A, Jr., et al. Physiologic Medium Rewires Cellular Metabolism and Reveals Uric Acid as an Endogenous Inhibitor of UMP Synthase. Cell. 2017;169(2):258-72.e17.
70. Ichinose W, Cherepanov SM, Shabalova AA, Yokoyama S, Yuhi T, Yamaguchi H, et al. Development of a Highly Potent Analogue and a Long-Acting Analogue of

Oxytocin for the Treatment of Social Impairment-Like Behaviors. J Med Chem. 2019;62(7):3297-310.

71. de Oliveira GC, Kanamori KS, Auxiliadora-Martins M, Chini CCS, Chini EN. Measuring CD38 Hydrolase and Cyclase Activities: 1,N6-Ethenonicotinamide Adenine Dinucleotide (ε-NAD) and Nicotinamide Guanine Dinucleotide (NGD) Fluorescence-based Methods. Bio Protoc. 2018;8(14):e2938.

72. Higashida H, Egorova A, Higashida C, Zhong ZG, Yokoyama S, Noda M, et al. Sympathetic potentiation of cyclic ADP-ribose formation in rat cardiac myocytes. J Biol Chem. 1999;274(47):33348-54.

Main Figures

Figure 1

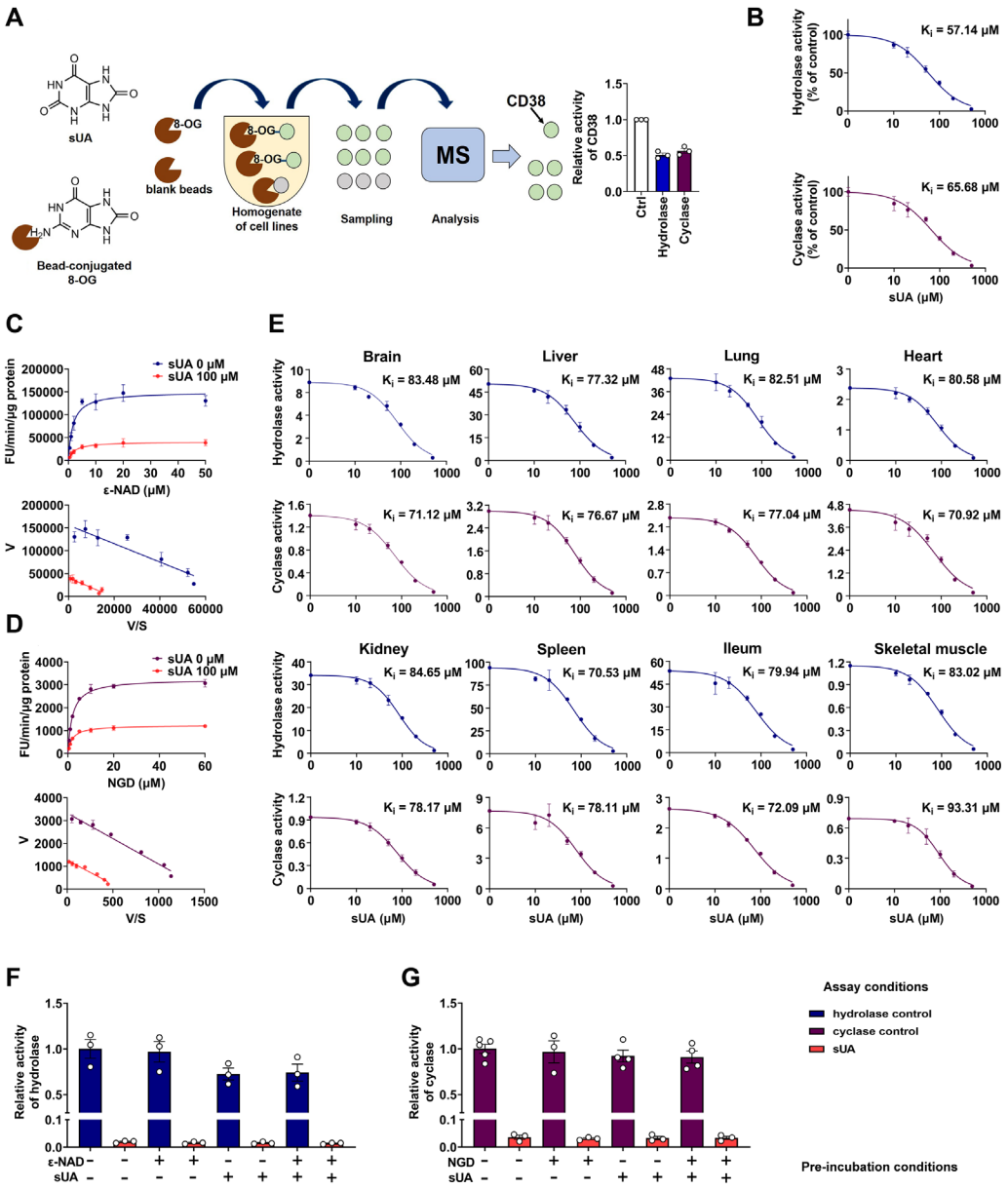

Figure 1. Identification of sUA as an endogenous inhibitor for CD38.

(A) Preliminary screening of 8-OG binding proteins by mass spectrum (MS)-based proteomics, and effect of 8-OG (50 μM) on CD38 activity. (n = 3 experiments/technical replicates).

(B) Hydrolase and cyclase activities of recombinant human CD38 (hCD38) in the presence of sUA, using nicotinamide 1, N^6-ethenoadenine dinucleotide (ε-NAD^+), and nicotinamide guanine dinucleotide (NGD) as substrates, respectively (n = 3 experiments/technical replicates).

(C and **D)** Effect of different substrate concentrations on sUA inhibition of recombinant hCD38 hydrolase (**C**) and cyclase (**D**) activities (n = 3 experiments/technical replicates).

(E) Effect of different sUA concentrations on hydrolase and cyclase activities (FU/min/μg protein) in tissues from 8- to 12-week-old WT mice (n = 3 mice).
(F and **G)** Reversibility of inhibition of recombinant hCD38 hydrolase (**F**) and cyclase (**G**) activities by sUA. After 30-min pre-incubation as indicated, samples were diluted 100-fold in reaction buffer with or without 500 μM sUA for enzyme assay (n = 3-5 experiments/technical replicates).
Data are mean ± s.d. (**B**-**E**) or mean ± s.e.m. (**A**, **F**, and **G**).
See also **Figure S1**.

Figure 2

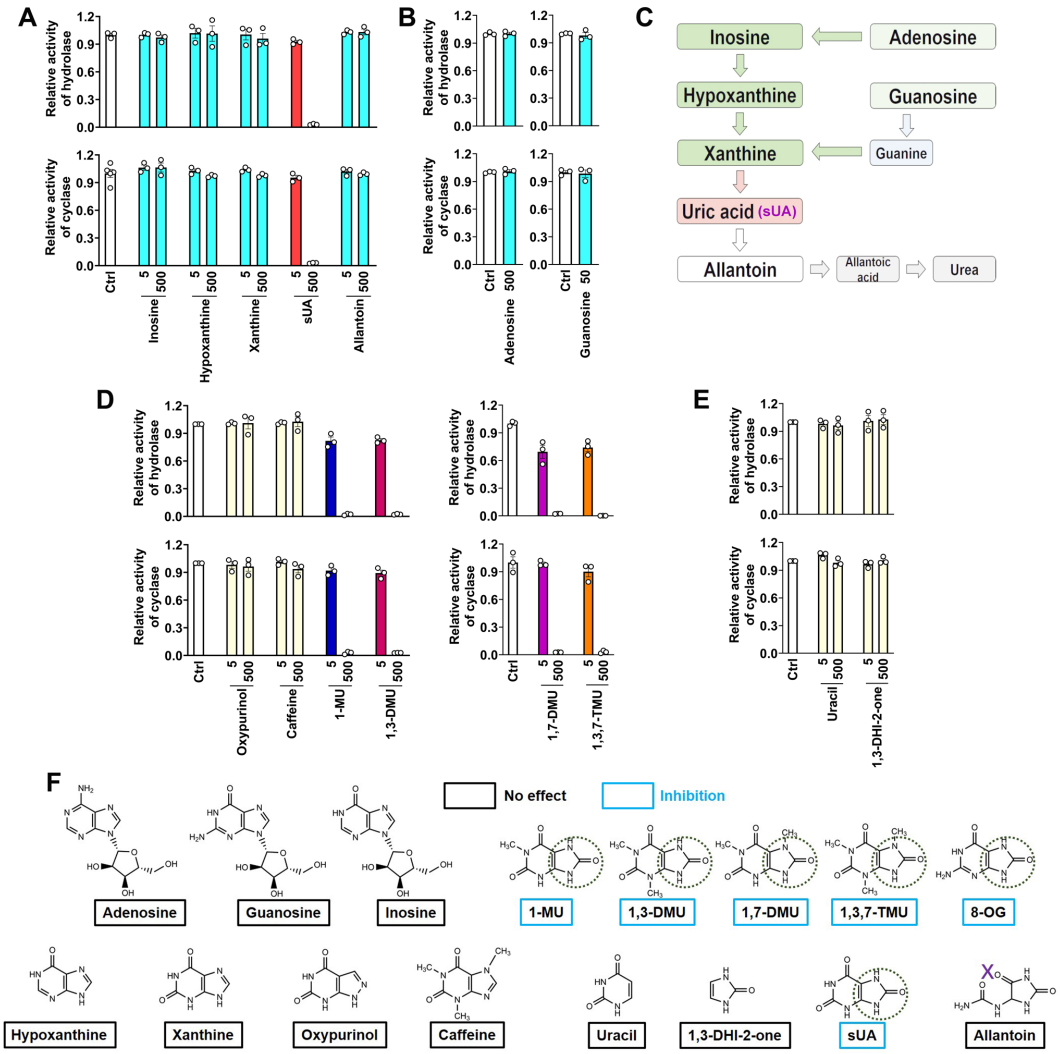

Figure 2. CD38 inhibition is restricted to sUA in purine metabolism.
(A and **B)** Effect of sUA precursors and metabolite on hydrolase and cyclase activities of recombinant hCD38 (n = 3 experiments/technical replicates for each ligand).
(C) Major pathways of purine metabolism.
(D) Effect of sUA analogs on hydrolase and cyclase activities (n = 3 experiments/technical replicates). THP-1 cells were used to detect the effects of oxypurinol, caffeine, 1-MU, and 1,3-DMU on hydrolase activity, recombinant hCD38 was used in the remaining detections.
(E) Effect of uracil and 1,3-dihydroimidazol-2-one (1,3-DHI-2-one) on hydrolase and cyclase activities of recombinant hCD38 (n = 3 experiments/technical replicates).
(F) A structural comparison reveals the functional group for CD38 inhibition.
The concentrations of all ligands are from 5 to 500 μM. Data are mean ± s.e.m.
See also **Figure S1**.

Figure 3

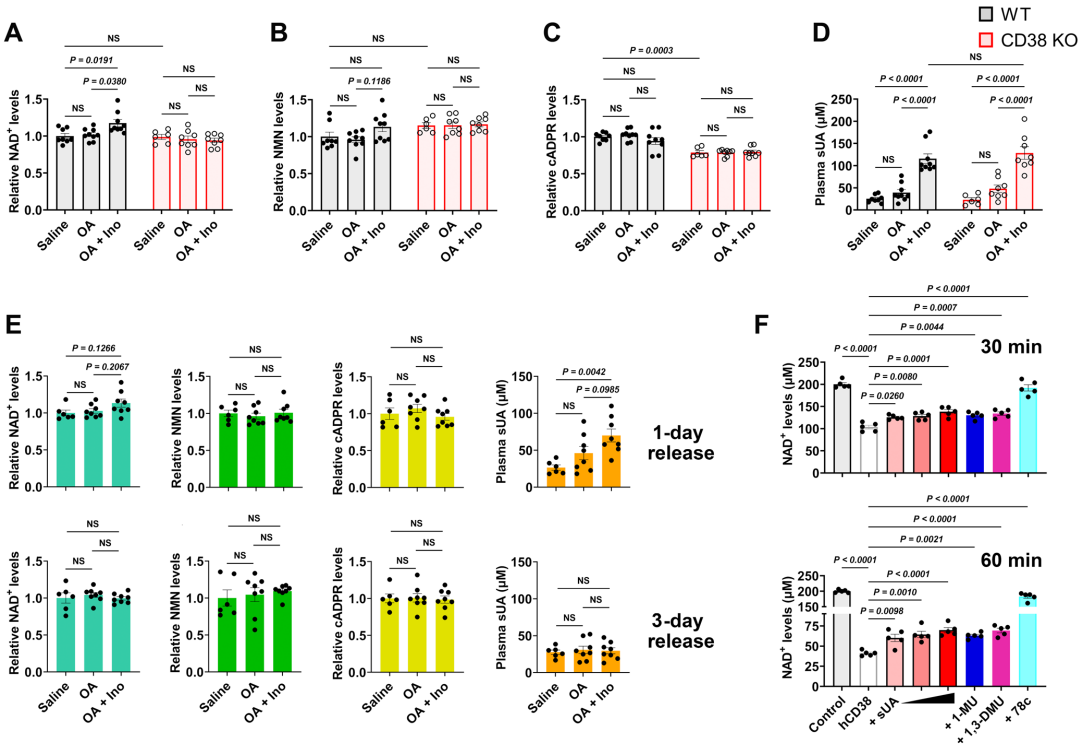

Figure 3. sUA physiologically limits NAD$^+$ degradation via CD38 inhibition.
WT and CD38 KO mice (10- to 12-week-old) received oral administration of saline, OA, or OA plus inosine (Ino) twice (1-day moderate sUA supplementation).
(A-D) Effect of 1-day sUA supplementation on whole blood NAD$^+$ (**A**), NMN (**B**), cADPR (**C**), and plasma sUA (**D**) levels in WT and CD38 KO mice (WT-Saline: n = 8 mice, WT-OA: n = 9 mice, WT-OA + Ino: n = 9 mice, KO-Saline: n = 6 mice, KO-OA: n = 8 mice, KO-OA + Ino: n = 8 mice).
(E) Effect of 1-day or 3-day release on whole blood NAD$^+$, NMN, cADPR, and plasma sUA levels in WT mice that received 1-day supplementation (WT-Saline: n = 6 mice, WT-OA: n = 8 mice, WT-OA + Ino: n = 8 mice).
(F) Effect of sUA (100, 200, or 500 μM) and other ligands (analogs at 500 μM, 78c, a CD38 inhibitor, at 0.5 μM) on NAD$^+$ degradation by recombinant hCD38 (n = 5 independent samples).
Data are mean ± s.e.m. Significance was tested using 2-way ANOVA (**A-D**), or 1-way ANOVA (**E** and **F**) with Tukey's multiple comparisons test. NS, not significant.
See also **Figures S1-S5** and **S7**.

Figure 4

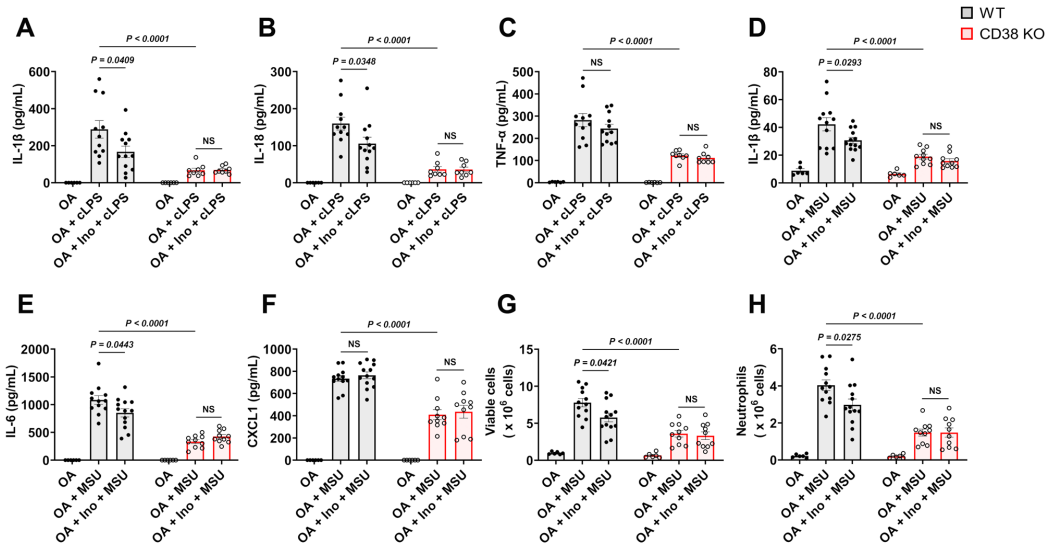

Figure 4. sUA physiologically prevents excessive inflammation by interacting with CD38.

WT and CD38 KO mice (10- to 12-week-old) received 1-day moderate sUA supplementation, plasma sUA was increased to the minimum physiological levels of humans in OA plus inosine groups. Then, the mice were stimulated with cLPS (2 mg/kg) or MSU crystals (2 mg/mouse) for 6 h.

(A-C) Effect of sUA at physiological levels on serum levels of IL-1β (**A**), IL-18 (**B**), and TNF-α (**C**) in mice with cLPS-induced systemic inflammation (WT-OA: n = 6 mice, WT-OA + cLPS: n = 11 mice, WT-OA + Ino + cLPS: n = 12 mice, KO-OA: n = 6 mice, KO-OA + cLPS: n = 8 mice, KO-OA + Ino + cLPS: n = 8 mice).

(D-H) Effect of sUA at physiological levels on IL-1β (**D**), IL-6 (**E**), and CXCL1 (**F**) levels and recruitment of viable cells (red blood cells excluded) (**G**) and neutrophils (**H**) in peritoneal lavage fluid from the mice with MSU crystal-induced peritonitis (WT-OA: n = 6 mice, WT-OA+MSU: n = 12 mice, WT-OA+Ino+MSU: n = 13 mice, KO-OA: n = 6 mice, KO-OA+MSU: n = 10 mice, KO-OA+Ino+MSU: n = 10 mice).

Data are mean ± s.e.m. Significance was tested using 2-way ANOVA with Tukey's multiple comparisons test. NS, not significant.

See also **Figures S3** and **S5-S9**.

Supplemental information

Functional identification of soluble uric acid as an endogenous inhibitor of CD38

Shijie Wen[1], Hiroshi Arakawa[1*], Shigeru Yokoyama[2,3], Yoshiyuki Shirasaka[1], Haruhiro Higashida[2], Ikumi Tamai[1,4*]

[1]Faculty of Pharmaceutical Sciences, Institute of Medical, Pharmaceutical and Health Sciences, Kanazawa University, Kanazawa, Japan

[2]Research Center for Child Mental Development, Kanazawa University, Kanazawa, Japan

[3]Division of Socio-Cognitive-Neuroscience, United Graduate School of Child Development, Osaka University, Kanazawa University, Hamamatsu University School of Medicine, Chiba University and University of Fukui, Kanazawa, Japan.

[4]Lead contact

[*]Correspondence: tamai@p.kanazawa-u.ac.jp (I.T.), arakawa@p.kanazawa-u.ac.jp (H.A.).

Figure S1

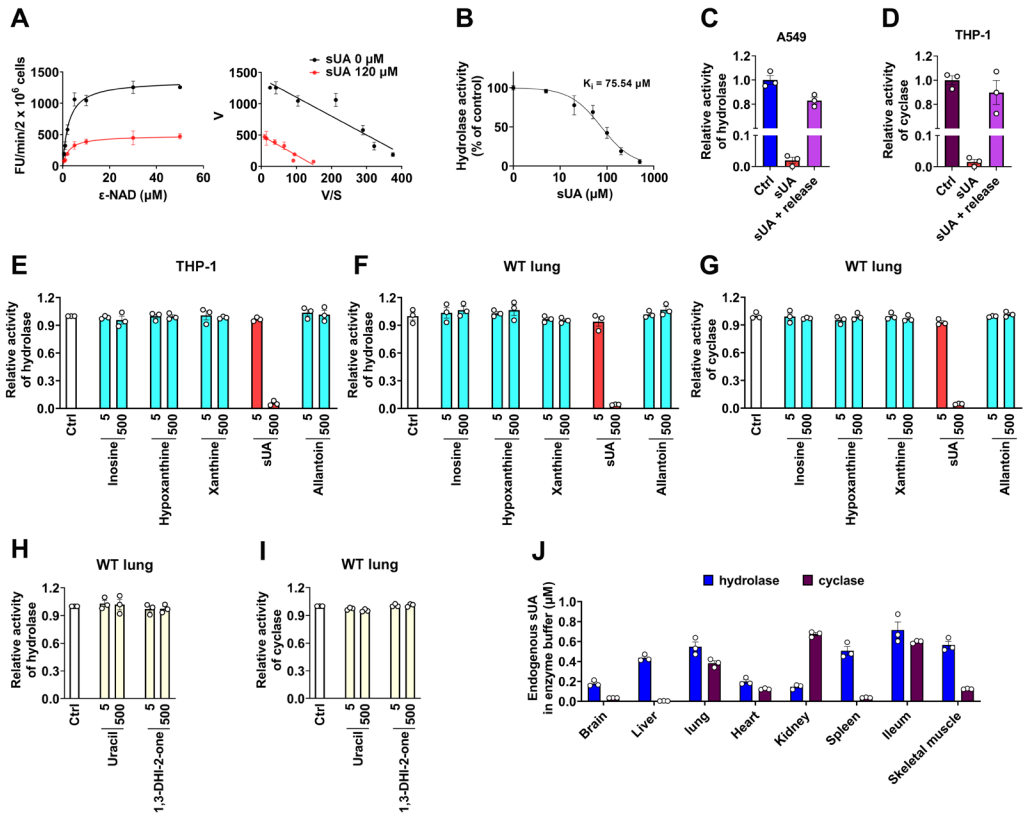

	Hydrolase Ki (μM)	Cyclase Ki (μM)	Tissue sUA (μmol/kg)
Brain	83.48	71.12	9.78
Liver	77.32	76.67	233.41
Lung	82.51	77.04	364.64
Heart	80.58	70.92	25.19
Kidney	84.65	78.17	26.01
Spleen	70.53	78.11	83.32
Ileum	79.94	72.09	226.24
Skeletal muscle	83.02	93.31	19.11

Supplemental Figure S1. Effect of sUA or other ligands on CD38 activity. Related to Figures 1-3.

(A) Effect of different ε-NAD$^+$ concentrations on sUA inhibition of hydrolase activity of THP-1 cells (n = 3 experiments/technical replicates).

(B) Hydrolase activity of THP-1 cells in the presence of sUA (0 to 500 μM) (n = 3 experiments/technical replicates).

(C and **D)** Reversibility of inhibition of hydrolase (A549 cells) (**C**) and cyclase (THP-1 cells) (**D**) by sUA (n = 3 experiments/technical replicates).

(E-G) Effect of sUA precursors and metabolite on hydrolase (**E** and **F**) and cyclase (**G**) activities. (n = 3 experiments/technical replicates)

(H and **I)** Effect of uracil and 1,3-dihydroimidazol-2-one (1,3-DHI-2-one) on hydrolase and cyclase activities of WT lung tissues. (n = 3 experiments/technical replicates)

(J) Endogenous sUA concentrations in the final reaction buffer for enzyme assays. sUA levels in initial homogenate or membrane fractions were measured, then the endogenous sUA concentrations in the final reaction buffer were calculated based on loading dilution (n = 3 biologically independent samples).

(K) Comparison between K_i values and mean levels of tissues sUA. K_i values were also

shown in Fig. 1E, and tissue sUA levels were from WT mice that received 1-day treatment of saline (also shown in Supplemental Fig. 2A).

(L and **M)** Hydrolase and cyclase activities of lung tissues from WT mice in the presence of OA (0 to 5 mM) (n = 3 experiments/technical replicates).

(N) Effect of OA administration on plasma sUA levels in WT mice that received oral administration of inosine. In saline group, the mice received oral administration and intraperitoneal injection of saline. In OA p.o. group, the mice received oral administration of inosine (1.5 g/kg) and OA (1.5 g/kg) (the same treatment in our models), and intraperitoneal injection of saline. In OA i.p. group, the mice received oral administration of inosine (1.5 g/kg), and intraperitoneal injection of OA (0.25 g/kg). Four hours after treatment, plasma sUA was measured (n = 5 mice per group).

Data are mean ± s.d. (**A, B, L,** and **M**) or mean ± s.e.m. (**C-J,** and **N**). Significance was tested using 1-way ANOVA with Tukey's multiple comparisons test (**N**).

Figure S2

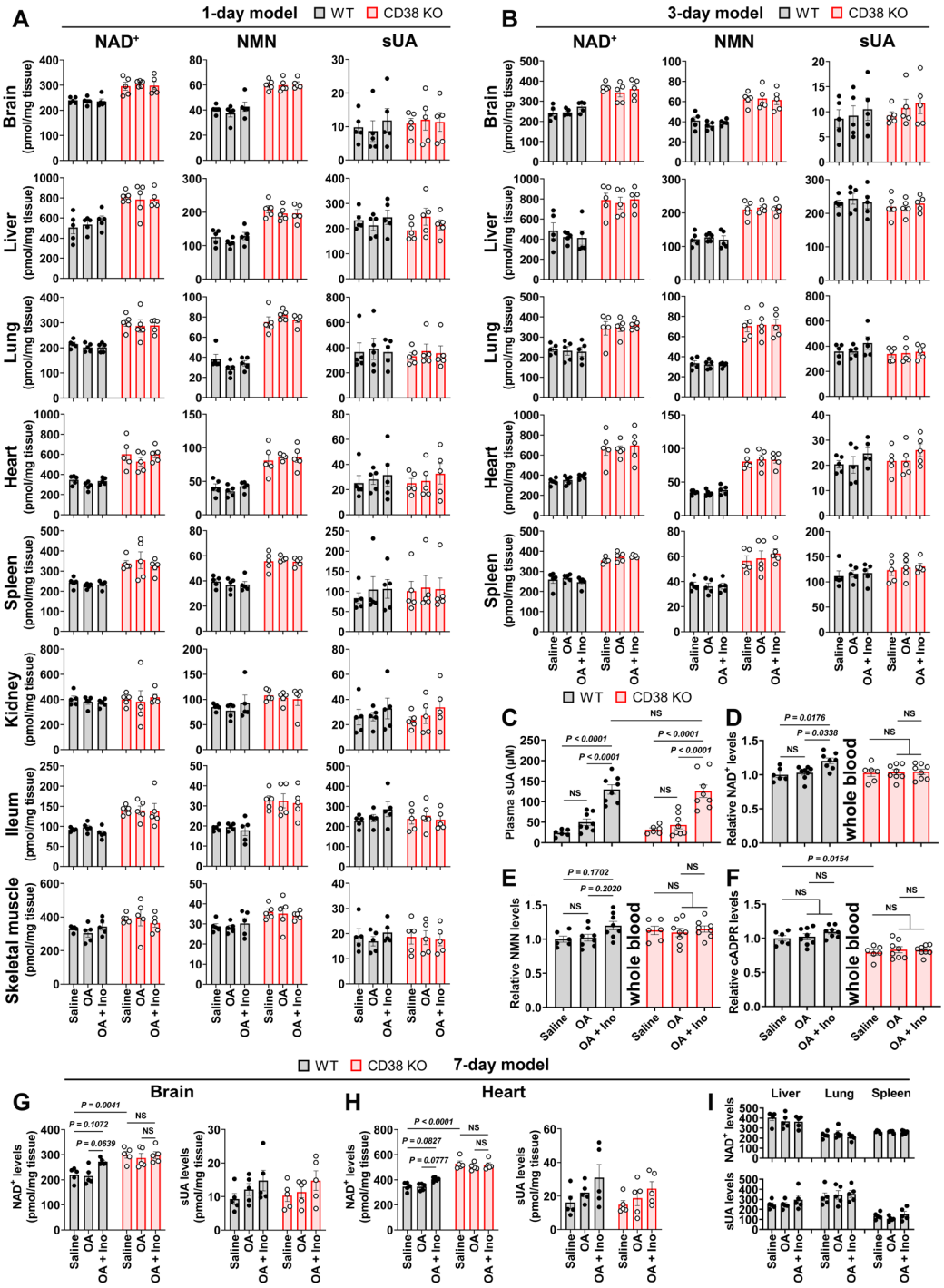

Supplemental Figure S2. Effect of moderate sUA supplementation on tissue NAD$^+$, NMN, and sUA levels. Related to Figure 3.

WT and CD38 KO mice (10- to 12-week-old) received oral administration of saline, OA, or OA plus inosine (Ino) twice daily for 1, 3, or 7 days. Four hours after the last treatment, the mice were sacrificed. In 1-day model, the mice were treated from the evening of day 0 to the morning of day 1.

(A) Effect of 1-day sUA supplementation on tissue NAD$^+$, NMN, and sUA levels (n = 5 male mice per group).

(B) Effect of 3-day sUA supplementation on tissue NAD^+, NMN, and sUA levels (n = 5 male mice per group).
(C-F) Effect of 3-day sUA supplementation on plasma sUA (**C**), whole blood NAD^+ (**D**), NMN (**E**), and cADPR (**F**) levels (WT-Saline: n = 6 mice, WT-OA: n = 8 mice, WT-OA+Ino: n = 8 mice, KO-Saline: n = 6 mice, KO-OA: n = 8 mice, KO-OA+Ino: n = 8 mice).
(G-I) Effect of 7-day sUA supplementation on tissue NAD^+ and sUA levels (n = 5 male mice per group).
Data are mean ± s.e.m. Significance was tested using 2-way ANOVA (**A-H**) with Tukey's multiple comparisons test or 1-way ANOVA (**I**) with Dunnett's multiple comparisons test.

Figure S3

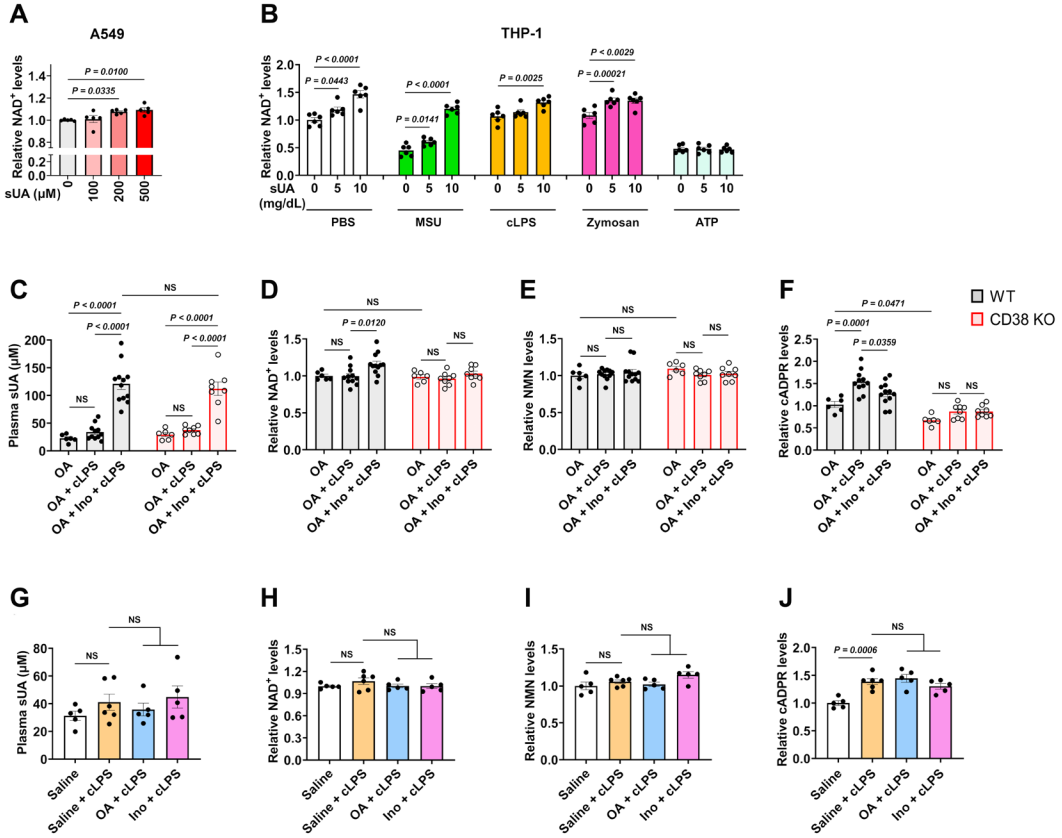

Supplemental Figure S3. Not OA or inosine but sUA limits NAD$^+$ degradation under inflammatory conditions. Related to Figure 3 and 4.

(A) Effect of sUA on intracellular NAD$^+$ levels of A549 cells (n = 5 biologically independent samples).

(B) Effect of sUA pre-incubation on intracellular NAD$^+$ levels of THP-1 cells. Naïve THP-1 cells were incubated with sUA (0-10 mg/dL) for 2h, then the cells were washed twice with PBS and stimulated with MSU crystals (200 μg/mL), cLPS (20 μg/mL), zymosan (50 μg/mL) or ATP (2 mM) for 6 h (n = 6 biologically independent samples).

(C-F) Effect of 1-day sUA supplementation on plasma sUA (**C**) and whole blood NAD$^+$ (**D**), NMN (**E**), and cADPR (**F**) levels in WT and CD38 KO mice under inflammatory conditions. The mice received 1-day sUA supplementation. Two hours after the last treatment, the mice were intraperitoneally stimulated with sterile PBS or cLPS (2 mg/kg) for 6 h (WT-OA: n = 6 mice, WT-OA+cLPS: n = 11 mice, WT-OA+Ino+cLPS: n = 12 mice, KO-OA: n = 6 mice, KO-OA+cLPS: n = 8 mice, KO-OA+Ino+cLPS: n = 8 mice).

(G-J) Effect of 1-day treatment of OA or inosine (Ino) on plasma sUA (**G**) and whole blood NAD$^+$ (**H**), NMN (**I**), and cADPR (**J**) levels in WT mice under inflammatory conditions. The mice received 1-day treatment of OA or Ino (from the evening of day 0 to the morning of day 1). Two hours after the last treatment, the mice were intraperitoneally stimulated with sterile PBS or cLPS (2 mg/kg) for 6 h (n = 6 mice in Saline+cLPS group, n = 5 mice in other groups).

Data are mean ± s.e.m. Significance was tested using 1-way ANOVA with Dunnett's (**A** and **B**) or Tukey's (**G-J**) multiple comparisons test, or 2-way ANOVA with Tukey's

multiple comparisons test (**C-F**).

Figure S4

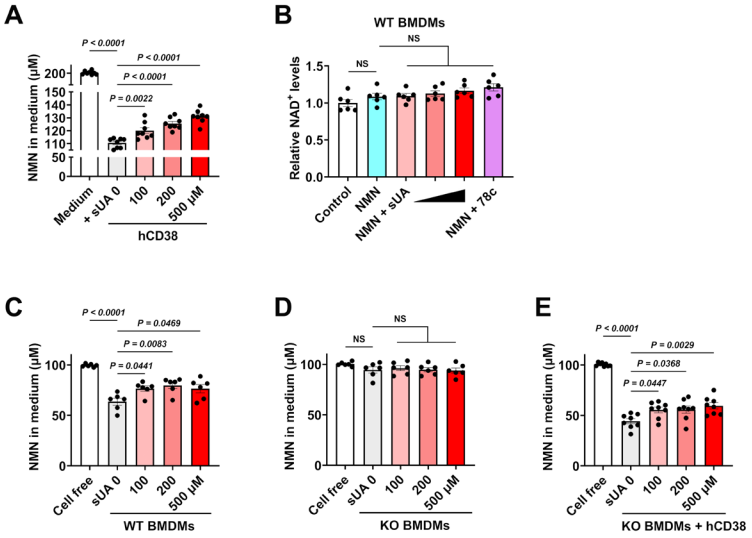

Supplemental Figure S4. sUA inhibits NMN degradation via CD38. Related to Figure 3.

(A) Effect of sUA on recombinant hCD38-mediated NMN (200 μM) degradation in medium (n = 8 independent samples).

(B) Effect of sUA (100, 200, and 500 μM) or 78c (0.5 μM) on intracellular NAD^+ levels of WT BMDMs treated with NMN. WT BMDMs were primed with100 ng/mL ultrapure LPS for 8 h (n = 6 biologically independent samples).

(C-E) Effect of sUA on extracellular NMN degradation in WT (**C**) or CD38 KO BMDMs in the absence (**D**) or presence (**E**) of recombinant hCD38 (10 ng/mL). BMDMs were primed with 100 ng/mL ultrapure LPS for 8 h before metabolic assays. (n = 6 biologically independent samples in **C** and **D**, n = 8 biologically independent samples in **E**)

Data are mean ± s.e.m. Significance was tested using 1-way ANOVA with Tukey's multiple comparisons test.

Figure S5

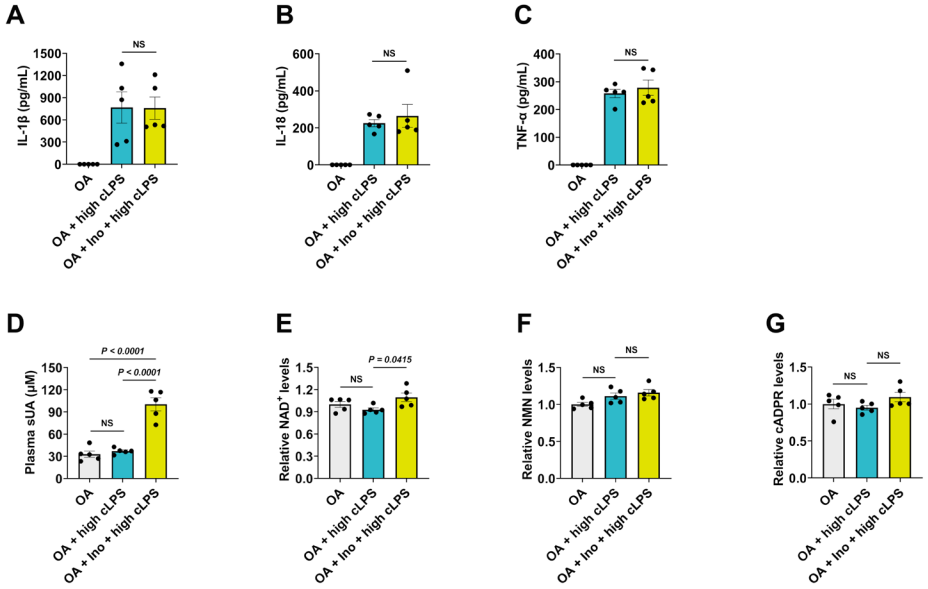

Supplemental Figure S5. Moderate sUA supplementation fails to prevent high-dose cLPS-induced systemic inflammation. Related to Figures 3 and 4.

WT mice received 1-day treatment of OA or OA plus inosine (Ino), 2 h after the last treatment, the mice were intraperitoneally stimulated with sterile PBS or cLPS (20 mg/kg) for 4 h (n = 5 mice per group).

(A-C) Serum IL-1β (**A**), IL-18 (**B**), and TNG-α (**C**) were measured.

(D-G) Plasma sUA (**D**), whole blood NAD^+ (**E**), NMN (**F**), and cADPR (**G**) levels were measured.

Data are mean ± s.e.m. Significance was tested using 1-way ANOVA with Tukey's multiple comparisons test.

Figure S6

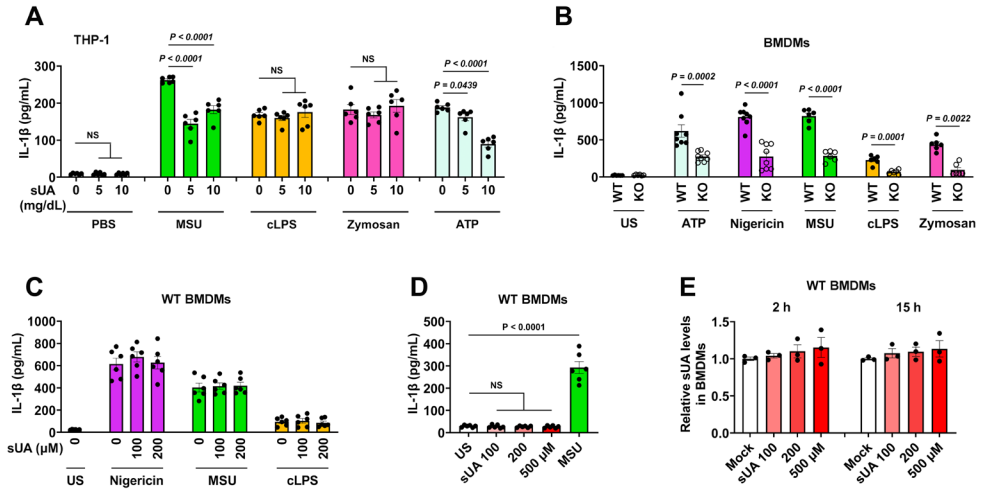

Supplemental Figure S6. Effect of sUA or CD38 KO on IL-1β release in primed THP-1 or BMDMs. Related to Figure 4.

(A) THP-1 cells were primed with 0.5 μM PMA for 3 h the day before stimulation. Primed THP-1 cells were pre-incubated with sUA (0-10 mg/dL) for 2 h, then the cells were washed twice with PBS and challenged by MSU crystals (200 μg/mL), cLPS (20 μg/mL), zymosan (50 μg/mL), and ATP (2 mM) for 4 h (n = 6 biologically independent samples).

(B) Effect of CD38 KO on IL-1β release in primed BMDMs. WT and KO BMDMs were primed with 100 ng/mL ultrapure LPS for 4 h, then primed BMDMs were challenged by ATP (5 mM, 30min), nigericin (3 μM, 2 h), MSU crystals (200 μg/mL, 6 h), cLPS (20 μg/mL, 6 h), and zymosan (50 μg/mL, 4 h). US means unstimulated. (n = 8 biologically independent samples in ATP and nigericin groups, n = 6 biologically independent samples in other groups)

(C-E) Effect of sUA pre-incubation on IL-1β release and intracellular sUA levels in primed BMDMs. WT BMDMs were primed with 100 ng/mL ultrapure LPS for 4 h. **(C)** The cells were pre-incubated with or without sUA (100 or 200 μM) for 2 h. Then, the cells were washed twice with PBS and were stimulated with nigericin (3 μM, 2 h), MSU crystals (200 μg/mL, 4 h), or cLPS (1 μg/mL, 4 h). (**D** and **E)** Primed BMDMs were directly incubated with sUA (100, 200, and 500 μM) or MSU crystals (100 μg/mL) for 6 h in **D**, 2 or 15 h in **E**. US means unstimulated. (n = 6 biologically independent samples in **C** and **D,** n = 3 biologically independent samples in **E**)

Data are mean ± s.e.m. Significance was tested using 1-way ANOVA with Dunnett's (**A** and **C-E**) multiple comparisons test, or two-tailed unpaired t-test and Mann-Whitney test (ATP and Zymosan) (**B**).

Figure S7

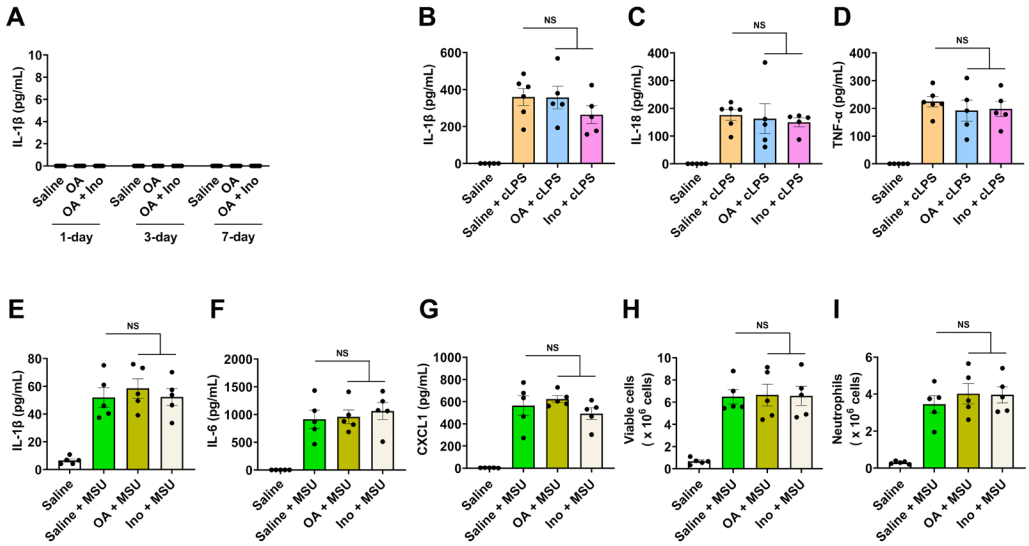

Supplemental Figure S7. OA or inosine alone does not limit cLPS-induced systemic inflammation and MSU crystal-induced peritonitis. Related to Figure 3 and 4.

(A) No effect of 1- to 7-day sUA supplementation on serum IL-1β levels (n = 5 mice per group).

(B-I) WT mice received 1-day oral administration of saline, OA, or inosine (Ino), 2 h after the last treatment, the mice were intraperitoneally stimulated with sterile PBS, cLPS (2 mg/kg), or MSU crystals (2 mg/mouse) for 6 h. **(B-D)** Serum IL-1β (**B**), IL-18 (**C**), and TNF-α (**D**) levels in mice with cLPS-induced systemic inflammation were measured (n = 6 mice in Saline+cLPS group, n = 5 mice in other groups). **(E-I)** IL-1β (**E**), IL-6 (**F**), CXCL-1 (**G**), and the number of viable cells (red blood cells excluded) (**H**) and neutrophils (**I**) in peritoneal lavage fluid from the mice with MSU crystal-induced peritonitis were measured (n = 5 mice per group).

Data are mean ± s.e.m. Significance was tested using 1-way ANOVA with Dunnett's (**A**) or Tukey's (**B-I**) multiple comparisons test.

Figure S8

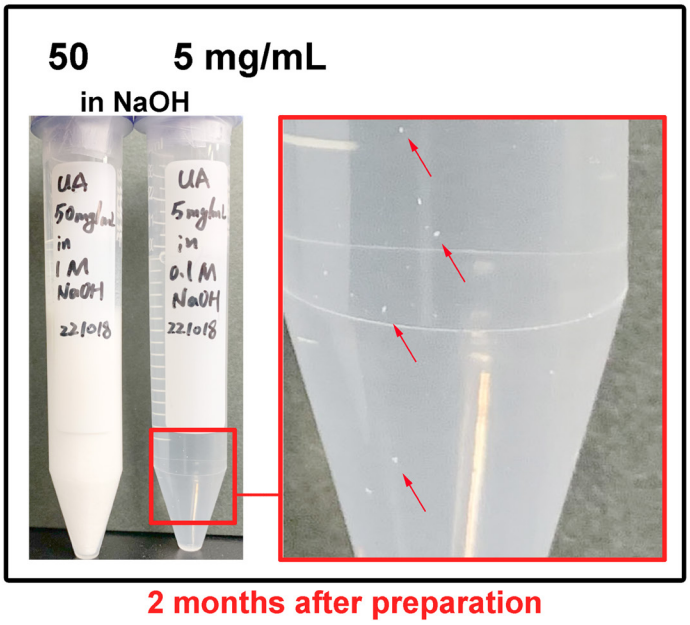

Supplemental Figure S8. Crystals precipitation in sUA stock solution. Related to Figure 4.

sUA stock solutions in NaOH were prepared without pH adjustment. Crystals were immediately precipitated after dissolution in 50 mg/mL tube. Visible crystals were observed in 5 mg/mL tube after 2-month storage at 4 °C.

Figure S9

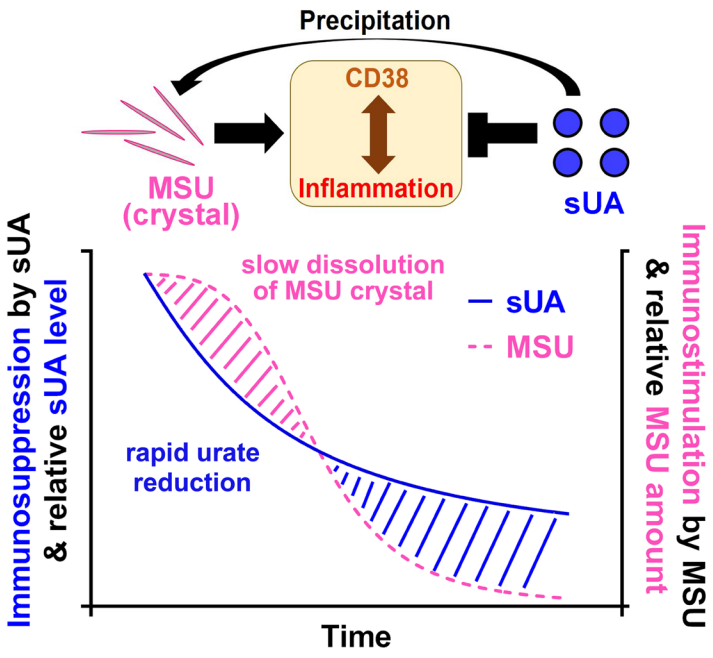

Supplemental Figure S9. Potential mechanism of the paradox in gout therapy. Related to Figure 4.

Table S1

MATERIALS and REAGENTS	SOURCE	IDENTIFIER
Chemicals, peptides, and recombinant proteins		
Uric acid	Sigma-Aldrich	Cat#U0881
β-Nicotinamide Adenine Dinucleotide (NAD+)	Nacalai	Cat#24338-86
β-Nicotinamide mononucleotide (NMN)	BLD Pharmatech	Cat#BD116593
cADP-Ribose (cADPR)	Santa Cruz	Cat#sc-201512
FYU-981	Fuji Yakuhin Co., Ltd.	N/A
78c	Sigma-Aldrich	Cat#5.38763
N-cyclohexyl benzamide	Sigma-Aldrich	Cat#R531332
Inosine	Nacalai	Cat#07139-42
Hypoxanthine	Sigma-Aldrich	Cat#H-9636
Xanthine	Sigma-Aldrich	Cat#X0626
Allantoin	Sigma-Aldrich	Cat#A-7878
Adenosine	FUJIFILM Wako	Cat#010-10491
Guanosine	FUJIFILM Wako	Cat#079-01111
Uracil	FUJIFILM Wako	Cat#212-00062
1,3-dihydroimidazol-2-one	BLD Pharmatech	Cat#BD00733674
Oxypurinol	Sigma-Aldrich	Cat#O-6881
Caffeine	FUJIFILM Wako	Cat#031-06792
1-methyluric acid	Sigma-Aldrich	Cat#M6885
1,3-dimethyluric acid	Santa Cruz	Cat#sc-206240
1,7-dimethyluric acid	Cayman Chemical	Cat#19584
1,3,7-trimethyluric acid	Cayman Chemical	Cat#16949
8-oxoguanine	Cayman Chemical	Cat#89290
Oxonic acid potassium salt	Sigma-Aldrich	Cat#156124
LPS from Escherichia coli 0111:B4 (crude LPS)	Sigma-Aldrich	Cat#L4130
Ultrapure LPS from Escherichia coli 0111:B4	InvivoGen	Cat#tlrl-3pelps
Phorbol 12-Myristate 13-Acetate	FUJIFILM Wako	Cat#162-23591
Nigericin	Sigma-Aldrich	Cat#N-7143
ATP	Oriental Yeast	Cat#45142000
Zymosan A from Saccharomyces cerevisiae	Sigma-Aldrich	Cat#Z4250
nicotinamide 1, N^6-ethenoadenine dinucleotide (ε-NAD+)	Sigma-Aldrich	Cat#N2630
nicotinamide guanine dinucleotide (NGD)	Sigma-Aldrich	Cat#N5131
Recombinant human CD38 protein	Sino Biological	Cat#10818-H08H
Recombinant human M-CSF protein	Proteintech Group	Cat#HZ-1192
Critical commercial assays		
Human IL-1β ELISA Kit	R & D Systems	Cat#DY201
Mouse IL-1β ELISA Kit	R & D Systems	Cat#SMLB00C
Mouse IL-6 ELISA Kit	R & D Systems	Cat#DY406-05

Mouse IL-18 ELISA Kit	R & D Systems	Cat#DY7625-05
Mouse TNF-a ELISA Kit	R & D Systems	Cat#DY410-05
Mouse CXCL1 ELISA Kit	R & D Systems	Cat#DY453-05
Wright-Giemsa Stain Kit	ScyTek Laboratories	Cat#WGK-1
Experimental models: Cell lines		
A549	ATCC	CCL-185
THP-1	ATCC	TIB-202
ICR bone marrow-derived macrophages	This paper	N/A
Experimental models: Organisms/strains		
ICR mice	Japan SLC, Inc.	N/A
CD38 KO ICR mice	Dr. Haruhiro Higashida, Kanazawa University	N/A
Software and algorithms		
Prism 9	GraphPad Software	https://www.graphpad.com
Labsolutions software (version 5.97)	Shimadzu	https://www.shimadzu.com/
Other		
RF-6000 Spectrofluorophotometer	Shimadzu	https://www.shimadzu.com/
LC-30A system	Shimadzu	https://www.shimadzu.com/
LCMS-8050	Shimadzu	https://www.shimadzu.com/